I.U.S.S.
Istituto Universitario
di Studi Superiori

Università degli
Studi di Pavia

**EUROPEAN SCHOOL OF ADVANCED STUDIES IN
REDUCTION OF SEISMIC RISK**

ROSE SCHOOL

EQUIVALENT VISCOUS DAMPING EQUATIONS FOR DIRECT DISPLACEMENT BASED DESIGN

**A Dissertation Submitted in
Partial Fulfilment of the Requirements for the
Master Degree in Earthquake Engineering**

By

Carlos Andres Blandon U

Advisors:
Prof. Nigel Priestley
Prof. Michele Calvi
Dr. Rui Pinho

October, 2004

ABSTRACT

Estimation of the equivalent viscous damping factor (EVDF) is an important step in the methodology of the direct displacement based design. The dynamic response of the substitute structure is characterized by an effective stiffness and an equivalent viscous damping, simplifying considerably the dynamic problem and making this approach very desirable for design purposes. However, errors in the estimation of these parameters characteristics lead to consequent errors in the ductility demand of the designed elements.

The most used procedure to estimate the equivalent viscous damping is the Jacobsen's approach, which estimates this factor based on the ratio between the elastic stored energy and the dissipated energy by a given hysteretic model. However this approximation assumes complete loops under a sinusoidal excitation (steady-state harmonic response). The real situation during an earthquake is different given that the complete loops are not formed in each cycle and the system is subjected to a random excitation.

Evidence from past investigations has shown that the Jacobsen approach can estimate, for some hysteretic models, the EVDF with the same accuracy as more elaborated techniques such as Gulkan's approach. This technique balances the input energy from the earthquake and the energy necessary to bring the system to rest using viscous damping. However, there are also investigations that indicate that Jacobsen's approach overestimates the value of the damping for some hysteretic models and for some earthquake characteristics such us pulses. Thereafter it is needed to carry out additional analyses to find the limitations of this approach.

A comparison of the displacements obtained from a non-linear time-history analysis and a spectral design was carried out for a specific single degree of freedom system (SDOF), in order to evaluate how accurate can these displacement be estimated using Jacobsen's approach. This procedure was repeated for six different hysteretic rules which covered a wide range of energy dissipation: a thin and a fat Takeda model, a bilinear model with high post yielding stiffness, an elastic perfectly plastic model, a Ramberg Osgood type model and a ring spring model. Six records were used, one synthetic, adjusted to a EC8 type target spectrum and five artificial records adjusted to Caltrans design spectra for soil type C (PGA=0.7g). The SDOF model was designed for five different levels of ductility (2 to 6) and effective periods from 0.5 to 4 s in steps of 0.5s. In iterative methodology was carried out until the displacements from the non-linear time-history analysis matched the design displacement obtained from the damped response spectra. In

order to separate the effects of elastic-viscous and hysteretic damping the designs and analyses were carried without elastic viscous damping.

It was found that in general the Jacobsen approach overestimates the values of the equivalent viscous damping with a few exceptions; As a consequence, modified equations were proposed in order to estimate the EVDF.

ACKNOWLEDGEMENTS

I would like to express my sincere gratitude to my advisors for their support and time dedicated. Their opinions and inputs help me to understand more deeply all the steps of the research and also to carry out a more conscientious and accurate work.

I also would like to thank Ing. Rishmilla Mendis and Dr. Julian Bommer of Imperial College, London,U.K. for their support and hard work specially dedicated to generate input data for this work.

I am also thankful to the people who gave me the opportunity to spend valuable time here at the ROSE school and that keep working to improve the institution day by day.

I am grateful for the support and time from the ROSE school students and friends which always have help me with their discussions and advises.

Finally I have to thank the support of my wife, family and friends which encourage me every day to keep on improving. But most of all, thanks to God which gives me the strength and life to go ahead and the opportunity to enjoy learning about his creation.

EQUIVAENT VISCOUS DAMPING EQUATIONS FOR DIRECT DISPLACEMENT BASED DESIGN

INDEX

LIST OF TABLES

LIST OF FIGURES

1 INTRODUCTION

Recent earthquakes (Northridge, Kobe, etc) have produced a large amount of damages to structures, with a significant number of deaths and high money losses. In order to create methodologies which could be used to comply with defined performance levels, limiting and evaluating more accurately the level of damage the philosophy of the performance based design has been developed. [Vision 2000]

Methodologies based on forces have generally been used, in the past, to define the capacity and demand of the structural systems under seismic excitation. However, it is now generally accepted that design methodologies based on displacement are more appropriated, and can overcome inherent deficiencies of traditional force based design. One of the main reasons is because the damage is more related to relative displacements than to forces. One of the alternatives of the methodologies based on displacement is "Direct Displacement Based Design (DDBD)" proposed by Priestley [Priestley 1994]. The basic concept and the methodology are outlined in the next chapter.

The accurate estimation of maximum displacements is then a key issue in the DDBD approach in order to obtain a reliable design of the elements. This is because if the real displacements are higher than the design displacements the elements would suffer a larger ductility demand than expected and in consequence larger level of damage risking local or global instability.

The system's maximum displacements may be obtained using different techniques but those of interest in this study are the non-linear time-history analysis and the modal analysis (from displacement response spectra) for different levels of damping. The former method is generally not used in design practice and it is preferred to use simplified methods such us the last one. However, in order to take into account the non-linear behaviour of the system when the modal analysis is used, it is necessary to use simplifications of the non-linear dynamic problem. Those will be explained in the next chapter.

However, in order to introduce the problem of this study, one of the simplifications mentioned in the previous paragraph will be mentioned beforehand. It relates to the issue of how the energy dissipation due to the non-linear behaviour can be taken into account into the linear response spectrum. This is done by simply applying an equivalent viscous damping factor (chapter 3) in order to obtain a reduced or "damped" displacement response.

The key step of the relationship between that dissipated energy due to the non-linear behaviour and the equivalent viscous damping is the main topic of this study. In actual practice, a relationship that has been obtained considering some theoretical assumptions has been used. However it is necessary to analyze how accurate are these assumptions for different types of earthquakes, structural periods (effective periods), ductility levels and structural systems (hysteretic models). Additionally, the effect on the response in terms of displacement will be studied.

The main objective is to review the existing equations used to estimate the equivalent viscous damping factor and if necessary, develop a general or a set of equations for such factor for different hysteretic models, ductility levels and effective periods. Such hysteretic models represent the general behaviour of the most common structural systems.

Given that it will be necessary to use time-history analysis for a given set of structural models using a set of earthquake records, it will be seen that the results obtained in this study are applicable for some specific conditions of initial viscous damping. This condition is important because it has been found that the selection of this parameter may influence significantly the response of the system. A parallel study that has been carried out by different authors [Grant and Priestley, 2004] will try to give an answer to this limitation, so that it can be overcome in future studies.

The document is divided in seven part which starts introducing the reader from the basic concepts of DDBD in chapter two and the concept of viscous damping and equivalent viscous damping in chapter three. Then, chapter four explains the methodology used to estimate the equivalent viscous damping. Chapter five contains the methodology carried by Mendis and Bommer [2004] in order to obtain and spectra compatible synthetic accelerogram and a set of artificial accelerograms adjusted to match a specific Caltrans displacement design spectra. In chapter six there is a description of the hysteretic models used in the analyses. The modelling assumptions and the results of the analyses are included in chapter seven and finally, chapter eight discuss the proposals made in order to estimate the EVDF in a more accurate way.

2 FUNDAMENTALS OF DIRECT DISPLACEMENT BASED DESIGN

The procedure is based on the concept of the substitute structure proposed by Shibata and Sozen [1976]. The structure is represented by an equivalent SDOF structure with equivalent system, mass and damping. The basic idea is to obtain the base shear from a given target displacement and the level of ductility that can be estimated from the section of the element. In this approach, structures are designed to achieve, rather than be limited by, displacements corresponding to a specified limit state

Step 1: Select a target displacement (Δ_C) of the structure based on considerations of the performance level, which change according to the use of the structure, code drift limit, or limit plastic rotation based on maximum strain levels. For Multi degree of freedom (MDOF) structures it is necessary to transform this displacement as described in step 2. For SDOF the next step is not necessary.

Step 2: For MDOF structures the problem is reduced into a SDOF system (Figure 2-1 (a)) with a target displacement (Δ_d) at a given equivalent height (H_e) and equivalent mass (m_e). [Priestley,2003]

$$\Delta_d = \frac{\sum_{i=1}^{n}\left(m_i \Delta_i^2\right)}{\sum_{i=1}^{n}\left(m_i \Delta_i\right)} \qquad \textbf{(2-1a)}$$

$$\Delta_i = \phi_i \frac{\Delta_c}{\phi_c} \qquad \textbf{(2-1b)}$$

$$H_e = \frac{\sum_{i=1}^{n} m_i \Delta_i H_i}{\sum_{i=1}^{n} m_i \Delta_i} \qquad \textbf{(2-1c)}$$

$$m_e = \sum_{i=1}^{n} \frac{m_i \Delta_i}{\Delta_d} \qquad \textbf{(2-1d)}$$

where ϕ_i is the inelastic mode shape which are often very similar to the elastic mode shape and can be obtained from approximated equations depending on the structural system and the structure height. m_i and Δ_i are the masses and displacements at each level of the MDOF structure.

Step 3: Calculate the level of viscous damping factor that is going to be used to reduce the elastic response spectra. This factor can be obtained from the ductility, which at the same time, has to be computed using the yielding displacement (Δ_y).

Δ_y is estimated from the assumed section of the elements based on the yielding curvature ϕ_y. Based on analytical and experimental results, Priestley [2003] have obtained approximate equation to compute ϕ_y .

Circular concrete column: $\phi_y = 2.25\varepsilon_y / D$ **(2-2 a)**

Rectangular concrete column: $\phi_y = 2.10\varepsilon_y / h_c$ **(2-3 b)**

Rectangular concrete wall: $\phi_y = 2.00\varepsilon_y / l_w$ **(2-4 c)**

Symmetrical steel section: $\phi_y = 2.10\varepsilon_y / h_s$ **(2-5 d)**

Flanged concrete beam: $\phi_y = 1.70\varepsilon_y / h_b$ **(2-6 e)**

where ε_y is the yield strain of the flexural reinforcement ($=f_y/E_s$), and D, h_c, l_w, h_s and h_b are the section depths of the circular column, rectangular column, rectangular wall, steel section and flanged concrete beam sections respectively.

For a SDOF vertical cantilever, such as a bridge pier, or a low rise cantilever wall, the yield displacement is given by Eq. (2-7).

$$\Delta_y = \phi_y H^2 / 3 \quad \textbf{(2-7)}$$

For reinforced concrete and structural steel frames, the yield drift can be developed from the yield curvature expressions Eq. (2-8a) as

Reinforced concrete frame: $\theta_y = 0.5\varepsilon_y l_b / h_b$ **(2-8a)**

Structural steel frame: $\theta_y = 0.6\varepsilon_y l_b / h_b$ **(2-8b)**

where l_b is the beam span, and h_b is the concrete or steel beam depth.

Ductility $\mu = \Delta_d / \Delta_y$ **(2-9)**

Where Δ_d is the maximum displacement and Δ_y is the yielding displacement.

Once this ductility is obtained it is possible to correlate it with an equivalent level of viscous damping. This value depends also on the structural system as shown in Figure 2-1 (c). There are multiple expressions proposed by different authors (see section 3.4). However, there are some shortcomings that need to be analyzed.

Step 4: The effective period of the structure can be obtained for the target displacement and the reduced design spectrum for the equivalent viscous damping level obtained in the previous step (Figure 2-1 (d)).

Step 5: From the effective period it is possible to obtain the effective stiffness of the equivalent SDOF system as shown by Eq. (2-10):

$$K_e = 4\pi^2 m_e / T_e^2 \tag{2-10}$$

where m_e is the effective mass of the structure participating in the fundamental mode of vibration. The design lateral force, which is defined by Eq. (2-11)

$$F = V_B = K_e \Delta_d \tag{2-11}$$

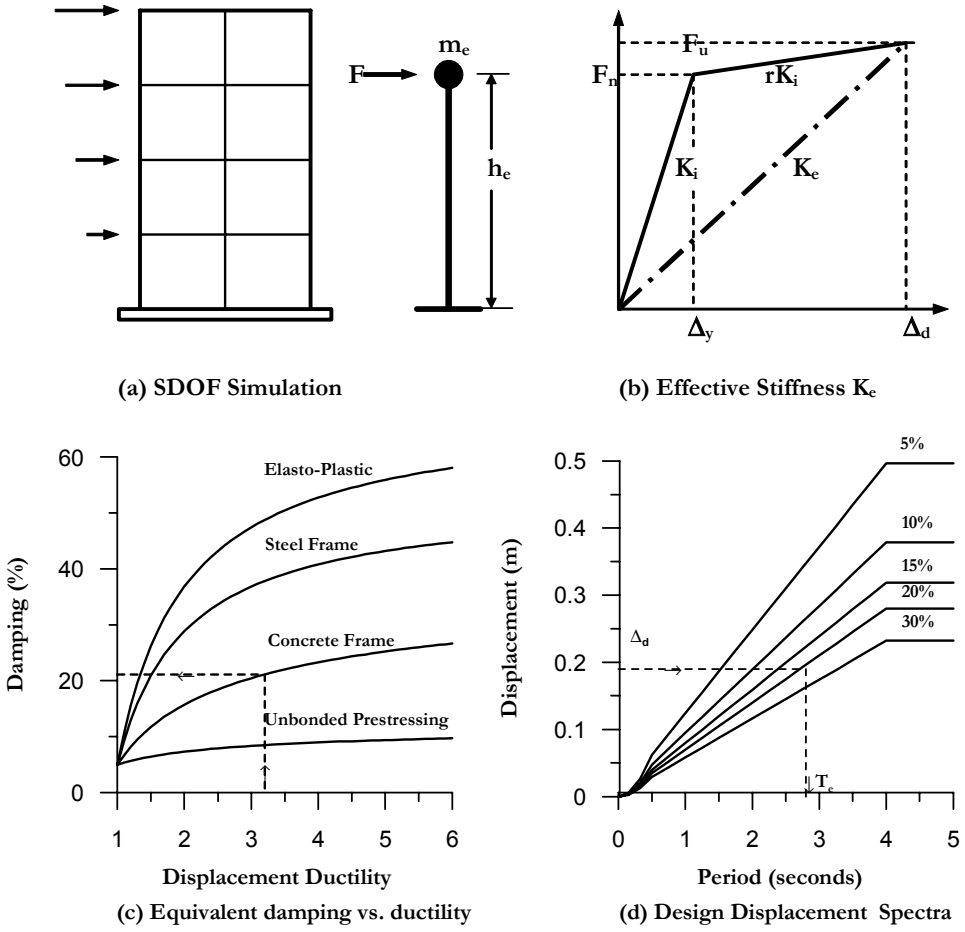

Figure 2-1 Fundamentals of Direct Displacement-Based Design [from Priesteley,2003]

As mentioned previously, the scope of the study is to revise and adjust the relationships used to estimate the equivalent viscous damping from the ductility. This is because the present equations have been obtained for particular conditions that are not complying for real earthquakes. This issue is discussed in detail in the next chapter.

3 VISCOUS DAMPING

The concept of viscous damping is generally used to represent the energy dissipated by the structure in the elastic range. Such dissipation is due to various mechanisms such as cracking, nonlinearity in the elastic phase of response, interaction with non-structural elements, soil-structure interaction, etc. As it is very difficult and unpractical to estimate each mechanism individually, the elastic viscous damping represents the combined effect of all of the dissipation mechanisms. There is no direct relationship of such damping with the real physical phenomena. However, the adoption of the viscous damping concept facilitates the solution of the differential equation of motion represented by Eq.3-1.

3.1 INTRODUCTION

One of the fundamental concepts of the structural dynamics is response of an undamped free vibrating SDOF system which is described by the differential equation

$$m\ddot{u} + ku = 0 \qquad \textbf{(3-1)}$$

Where m is the mass, k is the stiffness and u is the displacement of the SDOF system. The solution of this equation in terms of displacement for particular initial conditions represents the response of the system. The maximum amplitude of the response is constant in time.

In order to represent real system where the maximum response decreases with time, an additional factor including damping of the system is introduced.

$$m\ddot{u} + c\dot{u} + ku = 0 \qquad \textbf{(3-2)}$$

where c is a damping coefficient. The proportionality to the velocity means that this factor represents a viscous damper. There are not any special physical reasons to model the damping using such an approach unless real viscous dampers are added to the structure; the main reason to represent the dynamic response of the damped free vibration SDOF system with this differential equation is the fact that it is easy to solve. Dividing Eq. (3-2) by m

$$\ddot{u} + 2\xi\varpi_n\dot{u} + \varpi_n^2 u = 0 \qquad \textbf{(3-3)}$$

where

$$\varpi_n = \sqrt{\frac{k}{m}} \qquad \textbf{(3-4)}$$

$$\xi = \frac{c}{2m\varpi_n} \quad \textbf{(3-5)}$$

ω_n is the natural vibration frequency (radians/sec) of the system and ξ is the damping ratio or fraction of critical damping. There are different types of movement depending on the value of ξ but given the properties of the structures, only the underdamped case ($\xi < 1$) is of interest.

As mentioned above, the assumption of viscous damping simplifies greatly the dynamic problem and this is the reason why in the direct displacement based design the non-linear behaviour has been also represented by an equivalent viscous damping factor (ζ_{eq}). Using Eq. (3-3) with an equivalent value of viscous damping representing both elastic and hysteretic energy dissipation it is possible to solve a simple linear system instead of a non-linear system which is more time and resource demanding for design applications.

3.2 EQUIVALENT VISCOUS DAMPING

An early proposal to model the inelastic behaviour with a parameter proportional to the velocity was made by Jacobsen [1930,1960]. He approximated the non-linear friction behaviour to a power of velocity. This was initially used to compute the response of single-degree-of-freedom-systems (SDOF) when subjected to sinusoidal loads. Housner [1956] and Jennings [1964] carried out some investigation in order to extent the concept to other hysteretic systems. The concept of equivalent viscous damping is explained briefly emphasising the main assumptions.

As a general start point, the equations that have been proposed by other authors (see 3.4) divide the viscous damping coefficient in two parts:

$$\xi_{eq} = \xi_o + \xi_{hyst} \quad \textbf{(3-6)}$$

where ξ_o corresponds to the initial damping in the elastic range and ξ_{hyst} correspond to the equivalent viscous damping ratio that represents the dissipation due to the non-linear (hysteretic) behaviour.

There are some procedures that have been used to estimate the viscous damping for the elastic case such us measuring the amplitude decay from real test in laboratories or real buildings [Chopra, 1995]. In practice the value for the coefficient range between 2% and 5%. However, this part of the equation is outside of the scope of this study (see section 7.2).

For the equivalent viscous damping corresponding to the hysteretic response, the concept of dissipated (E_{Diss}) and stored (E_{sto}) energy has been used [Jacobsen, 1930]. With reference to Fig 3.1, the value of the equivalent viscous damping ratio can be obtained equating the energy dissipated by a viscous damper with the energy dissipated from non-linear behaviour Eq. (3-7).

$$\xi_{hyst} = \frac{1}{4\pi} \cdot \frac{\varpi_n}{\varpi} \frac{E_{Diss}}{E_{sto}} \tag{3-7}$$

In order to use this approach it is necessary to assume that both systems are subjected to a harmonic excitation as describe by Eq. (3-8). This is necessary to ensure that the loops are complete and to obtain a closed-form solution for the displacement.

$$m\ddot{u} + c\dot{u} + ku = p_o \sin \varpi t \tag{3-8}$$

where ω is the frequency of the load and t is the time. The solution of this differential equation has two parts, however, only the part that represents the stabilized vibration (steady state) is taken into account as given in Eq. (3-9).

$$u(t) = u_o \sin(\varpi t - \phi)$$

$$\phi = \tan^{-1} \frac{2\xi\left(\varpi / \varpi_n\right)}{1 - \left(\varpi / \varpi_n\right)^2} \tag{3-9}$$

As shown in Figure 3-1 (a), the dissipated energy is equal to the area enclosed inside an entire loop. The elliptical loop is obtained from the equation that describes the energy dissipated by the viscous damper. Meanwhile, the hysteretic model (Figure 3-1 (b)) is used to represent the non-linear behaviour of an entire structural system. Depending on this system, the hysteretic model changes its characteristics and shape. In chapter 6 there is a description of the hysteretic models used in this study. The stored energy is also plotted by lines inside the triangle of the first quadrant (Figure 3-1) and can be obtained from Eq. (3-10).

$$E_{sto} = \frac{ku_o^2}{2} \tag{3-10}$$

The energy dissipated by the viscous damper can be expressed as the integral of the force of the damper (f_{damp}) by each differential displacement (du).

$$E_{Diss} = \int f_{damp} \cdot du = \int_0^{2\pi/\varpi} (c\dot{u})\dot{u} \cdot dt$$

Given that is assumed that the system is subjected to harmonic loading

$$E_{Diss} = c \int_0^{2\pi} [\varpi u_o \cos(\varpi t - \phi)]^2 \, dt = \pi c \varpi u_0^2$$

Hence

$$E_{Diss} = 2\pi\xi \frac{\varpi}{\varpi_n} k u_0^2 \tag{3-11}$$

When the areas inside the loops of Figure 3-1 are made equal and substituting Eq. (3-10) in Eq. (3-11) then Eq. (3-7) is obtained.

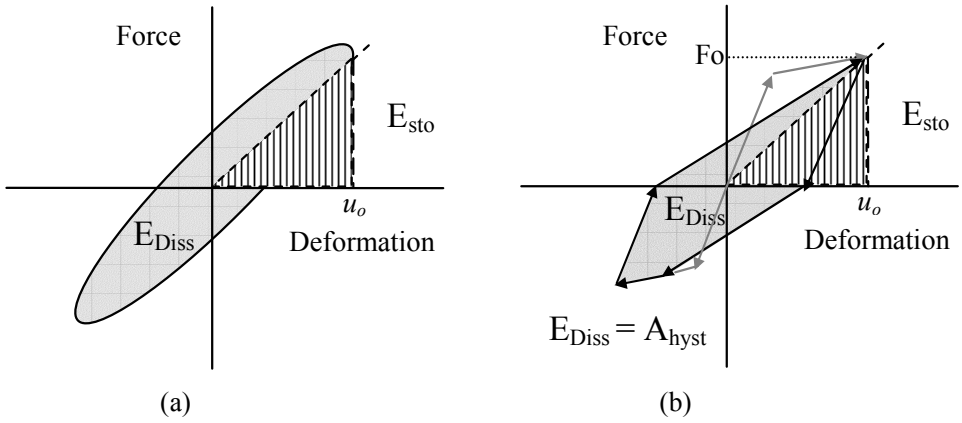

Figure 3-1. Dissipated and stored force for viscous damping (a) and hysteretic cycles (b)

Finally, it is assumed that the excitation frequency is the same as the natural frequency of the SDOF system (resonance condition), so the final equation is:

$$\xi_{hyst} = \frac{1}{4\pi} \cdot \frac{E_{Diss}}{E_{sto}} = \frac{1}{2\pi} \frac{A_{hyst}}{F_o u_o} \tag{3-12}$$

The equivalent damping of the structure has been defined based on the work of Jacobsen, for a sinusoidal response of a SDOF. It is clear, however, that response to real earthquake excitation cannot be exactly represented by steady-state harmonic response, and that an unknown error will be introduced in the estimation of displacements, based on the approximations made in Jacobsen's approach.

3.3 PREVIOUS RESEARCH

Gulkan and Sozen [1974] extended Jacobsen's approach by introducing the concept substitutive viscous damping (SVD) based on limited experimental results. They obtained the value of this factor for a given secant stiffness (effective period) and a given time-history by balancing the input energy of the SDOF with a linear dashpot that would bring the system to rest as described by Eq. (3-13):

$$\xi_{substitute} = \frac{T_{substitute} \int_0^t \ddot{u}_g \cdot \dot{u} \cdot dt}{4\pi \int_0^t \dot{u}^2 dt} \tag{3-13}$$

where u is the structure displacement, t is the total time of the accelerograms and $\ddot{u}_g$ is the ground acceleration. $T_{substitute}$ is the effective period corresponding to the secant stiffness to maximum response and $\xi_{substitute}$ is the SVD.

They also computed the same factor using the approximation by Jacobsen and they found out that the results were not significantly different. This indicated that practically there is no need to make extra efforts to compute the viscous damping factor, at least for the cases that they studied. However, more extensive analyses by Judi et al [2000] found significant differences between Jacobsen's Equivalent viscous damping factor, and Gulkan and Sozen's substitute damping factor, and concluded that designs based on the latter provided a better estimate of the expected displacement response.

Kowalsky and Ayers [2002] carried out a bibliographic investigation of research in the past aimed at obtaining the non-linear response of a SDOF system using equivalent damping factor and the period. For instance Iwan and Gates [1979] carried out several time-history analysis using initial period, ductility and ground motion as variables and the found that the equivalent viscous damping factor that would estimate the inelastic response of the SDOF system would not exceed 14%. Additionally, they found out that the peak displacement was relatively insensitive to the equivalent damping. (using a hysteresis model derived form a combination of elastic and Coulomb slip elements)

Kowalsky and Ayers [2002] also investigated the substitutive damping approach and tried to identify potential limitations and the range of applicability of the equivalent damping for the DDBD and based in the initial stage of the work they found that "on average, assessment of non-linear response with equivalent linear systems defined by effective period at maximum response and equivalent damping defined by Jacobsen's approach yields good results for the majority of cases considered". However they found that in cases with time histories with large pulses, the equivalent damping approach fails to recognize that the peak non-linear response is not longer a function of the energy dissipated. It is important to mention that only the Takeda degrading stiffness model was used in this work, changing the post yielding stiffness and stiffness degrading parameter. The velocity pulses phenomena was also pointed out by Priestley [2003] when he proposed a modified reduction equation for high damping spectral displacements for earthquakes containing large velocity pulses.

In conclusion, Kowalsky and Ayers, found that it is necessary to carry out additional investigation in order to find out the limits and variation of using this simplified assumption. The results obtained by Gulkan and Sozen, contrast with those obtained by Hudson [1965] and Judi [2000], which conclude that, at least for bi-linear oscillators, the equivalent damping factor underestimate the real response and the substitute viscous damping (SVD) gives better approximations. However, the use of the SVD is not practical, given that this value would be different for each earthquake record and it would be necessary to obtain a time-history response each time that the SVD is needed.

Regarding to the equivalent damping coefficient, some analysis were carried out in order to obtain the value of this variable that match the displacement and the equivalent period from the spectra and the time histories. A large scatter was found in the equivalent damping; such scatter is larger in the short periods than in the long periods. This means that the number of cycles is important in the damping since short periods structures will be subjected to a larger number of cycles than long period structures. Additionally, short period structures have smaller displacements than the long periods, so a slight variation of the displacement is much larger in proportion in the shorter periods.

Reasoning about the last paragraph, it could be possible to say that this behaviour is expected. This is because, as the damping increases, the effect on the displacement decreases (Figure 3-2).

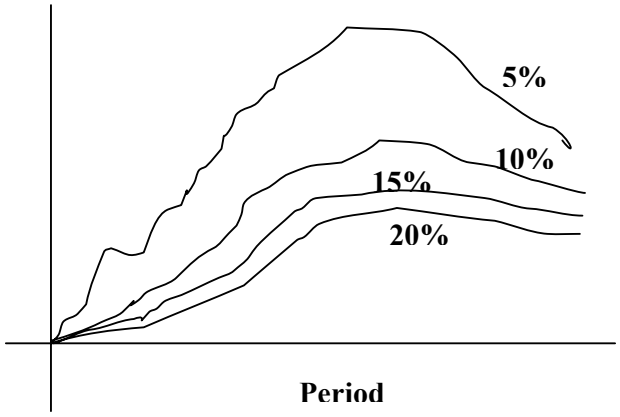

Figure 3-2 Effect of the viscous damping in the displacement spectra.

The effect of damping is even lower for cases where the time-history is characterized by velocity pulses. This was also observed by Kowalsky when he compared the response of different SDOF using the Pacoima dam Record and an artificial UBC matched record. In the former one, a large long duration acceleration pulse occurs early on in the record causing the structure to go inelastic with just a few or almost no oscillation, reducing significantly the capacity of the structure to dissipate energy by hysteresis.

The results obtained by Kowalsky are coherent with those obtained by Otani [1981] and Riddell et al [2002]. They carried out several time-history analysis using different hysteretic models. They found that if the parameters that described the hysteretic model were "equivalent" (initial stiffness, yielding force,etc) in order to obtain approximately the same ductility level, the displacements obtained for each model were very close among them. Once again, there seems to be a given level of independence of the response from the damping. However, it is necessary to review the limits of this independence and the level of uncertainty that the damping should be estimated for the DDBD design procedure.

In a more recent research, Kowalsky and Dwairi [2004] concluded that the Jacobsen approach frequently overestimated the damping and that the fundamental period of the system, the characteristics of the ground motion and the ductility level are critical variables for the equivalent damping concept.

Concluding from these researches, the equivalent damping deserves additional studies due to fact that it is practical use for design and there are still several uncertainties and contradictory results that need to be explained. It is necessary then, to find accurate expressions to estimate this parameter based on the kind of hysteretic loop and time-history records.

3.4 EXISTING EQUIVALENT VISCOUS DAMPING EQUATIONS

The DDBD is based on an equivalent SDOF system that represents the MDOF system. The non-linear behaviour of the structure is represented by a linearized equivalent SDOF (Figure 3-3) using the concept of the substitute structure [Shibata Sozen,1974].

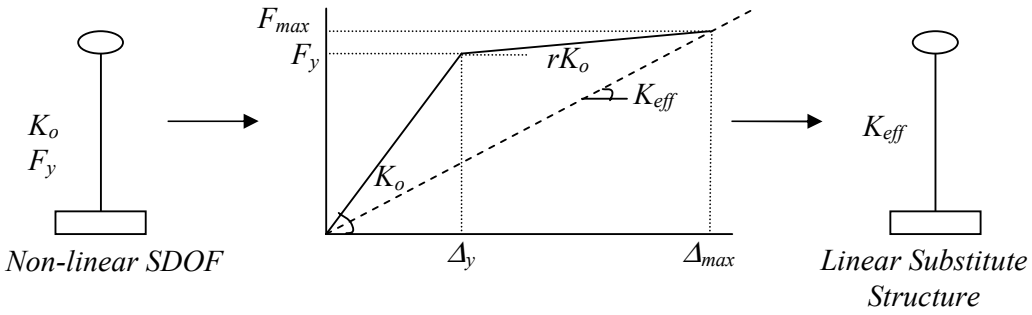

Figure 3-3 Substitute structure.

For a bilinear type hysteretic model, the initial stiffness (or initial period) and the yielding strength are the main parameters that need to be defined. In the paper by Miranda [2001], the equations proposed by Rosenblueth and Herrera in Eq.(3-14), and by Iwan in Eq. (3-15) define the relationship between the initial and effective periods for a given ductility level and post elastic stiffness coefficient. However, in the direct displacement based design the effective or equivalent period as defined by this equation is an input parameter that is already known.

$$\frac{T_{eq}}{T} = \sqrt{\frac{K_o}{K_s}} = \sqrt{\frac{\mu}{1-r+r\mu}} \quad \text{Rosenblueth and Herrera} \tag{3-14}$$

where r is the post-elastic stiffness coefficient.

$$\frac{T_{eq}}{T} = 1 + 0.121(\mu - 1)^{0.939} \quad \text{Iwan} \tag{3-15}$$

The difference in these equations is based on the fact that the results obtained by Rosenblueth were obtained analytically from the relationship between initial and secant stiffness for a given ductility and post-elastic coefficient, meanwhile, the results given by Iwan were obtained from a statistical evaluation

of a large number of inelastic analysis using systems and accelerograms with different characteristics. The effective damping estimated by the previous equations is shown in Figure 3-4. Even though it is not clear which characteristic used Iwan for his systems, it is clear that the effective period obtained with his equation is lower than that obtained by Rosenblueth. The *r* factor used for the last equation was 0.05, which would have to be increased to 0.3 in order to obtain approximately the same values estimated by Iwan's equation.

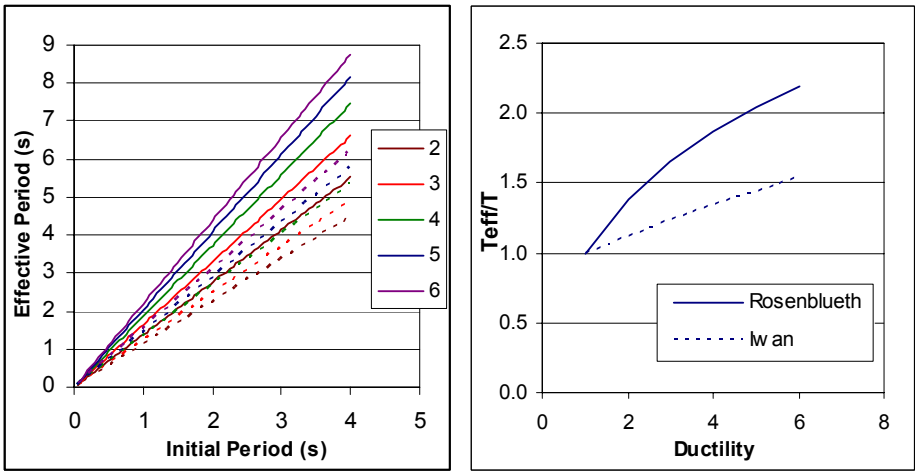

Series represent ductility level

Figure 3-4 Initial vs effective period relationship (Rosenblueth -continuous line; Iwan – dashed line).

However, the equations to obtain the effective period of the SDOF do not have practical use in the DDBD process given that this parameter is obtained from other parameters as explained in chapter 2 (Figure 2-1). It is important, however, the definition of the equivalent viscous damping.

There are multiple references which report different equations for the equivalent viscous damping factor Preistley[2003], Fardis and Panagiotakos[1996], Miranda and Ruiz [2002], Calvi [1999]. Some of the reported equations are shown afterwards.

Bilinear elasto-plastioc system, Rosenblueth and Herrera [1964]

$$\varepsilon_{eq} = \varepsilon_o + \frac{2}{\pi}\left[\frac{(1-r)(u-1)}{\mu - r\mu + r\mu^2}\right] \quad \textbf{(3-16a)}$$

Takeda Model, Gulkan Sozen [1974].

$$\varepsilon_{eq} = \varepsilon_o + 0.2\left(1 - \frac{1}{\sqrt{\mu}}\right) \quad \textbf{(3-16b)}$$

Elastic and Coulomb slip elements, Iwan[1980]

$$\varepsilon_{eq} = \varepsilon_o + 0.0587(\mu - 1)^{0.371} \quad \textbf{(3-16c)}$$

Takeda model α= 0.5 and β =0. Kowalsky [1994]

$$\varepsilon_{eq} = \varepsilon_o + \frac{1}{\pi}\left(1 - \frac{1-r}{\sqrt{\mu}} - r\sqrt{\mu}\right) \quad \textbf{(3-16d)}$$

Steel members, Priestley[2003]

$$\varepsilon_{eq} = 5 + \frac{150}{\mu\pi}(\mu - 1) \ \% \quad \textbf{(3-16e)}$$

Concrete frames, Priestley[2003]

$$\varepsilon_{eq} = 5 + \frac{120}{\pi}\left(1 - \frac{1}{\sqrt{\mu}}\right)\% \quad \textbf{(3-16f)}$$

Concrete columns, and walls, Priestley[2003]

$$\varepsilon_{eq} = 5 + \frac{95}{\pi}\left(1 - \frac{1}{\sqrt{\mu}}\right)\% \quad \textbf{(3-16g)}$$

Precast walls or frames, with unbonded prestressing Priestley[2003]

$$\varepsilon_{eq} = 5 + \frac{25}{\pi}\left(1 - \frac{1}{\sqrt{\mu}}\right)\% \quad \textbf{(3-16h)}$$

in general, the equations proposed by Priestley have the form

$$\xi_{eq} = \xi_o + a\left(1 - \frac{1}{\mu^{\beta}}\right) \quad \textbf{(3-17)}$$

where *r* is the post yielding stiffness coefficient, ξ_{eq} is the equivalent viscous damping factor, ξ_o is he initial viscous damping and μ is the ductility level. Some of these equations will be compared with those obtained by the methodology described in the next chapter. Figure 3-5 shows equivalent viscous damping obtained for each of the previous equations. *r* value for those equations which required it was set equal to 0.05. As can be observed, there are large variations depending on the system represented, i.e. the EVFD for linear elastic systems (Rosenblueth) gives the highest values meanwhile, the prestressed unbonded concrete (Priestley) gives the lowest values. There are significantly differences in the EVDF estimated for the concrete systems (Kowalsky, Gulkan, Concrete wall) which may affect the estimated displacement obtained form the design spectra.

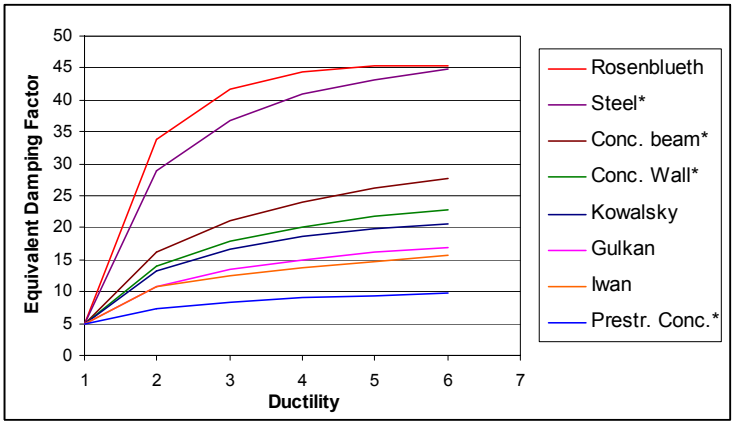

Figure 3-5 Equivalent viscous damping factor for (3-16a) to Eq. (3-16h). (* proposed by Priestley [2003]

Miranda (2002) carried out an investigation comparing the capabilities of different performance based methodologies in estimating the inelastic displacement for Takeda, modified Clough, stiffness degrading and elastoplastic system using 264 ground motion records. He classified these methodologies in two: Method based on equivalent linearization which use the equations proposed by Rosenblueth, Gulkan, Iwans and Kowalsky; and Method based on a displacement modification factor (Miranda, Newmark and Hall). For the scope of this study, only the results for the first class is discussed

It was found out the ratio between the time-history analyses and the design displacement from the linearized system changed according to the equation used to estimate the damping and the effective period. The equations proposed by Iwan produced the best results (ratios closer to one) and the lowest deviations followed in order by the equation proposed by Kowalsky, Gulkan and Rosenblueth. There is however, a significant inaccuracy for all the equations when predicting the displacement for short period systems ($T < 0.5$ sec). Additionaly, there are large dispersion in some particular cases, which means, as pointed out by Miranda, that if this equations are applied to individual ground motions they could lead to significant error in the estimation of the maximum inelastic displacement. This situation has been taken into account when the accelerograms and displacement spectra have been defined for this present work (see chapter 5). The findings of Miranda also suggest that it is necessary to carry out additional studies in order to find out the reason of this variability and improve the relationships used to estimate the viscous damping factor.

The studies mentioned above consistently indicated problems with use of Jacobsen's approach for equivalent viscous damping within DDBD methodology. However, rigorous analyses had not been carried out to optimise damping values applicable to a wide range of hysteretic models and period ranges. This study attempts such an optimization

4 METHODOLOGY FOR THE ESTIMATION OF THE EQUIVALENT VISCOUS DAMPING

Based on the results obtained from the previous research described in the previous section, a methodology was implemented, to modify where necessary Jacobsen's equations for the equivalent viscous damping factor (ξ).

The scope of the procedure is to determine the value of equivalent damping that has to be applied to an equivalent elastic system with a given effective period based on the secant stiffness to maximum displacement response in order to match its response (in terms of maximum displacement) to that obtained from a system with the same period (effective period) and a given level of ductility using non-linear time-history analysis. The final objective of this procedure was to develop equations that define the equivalent damping factor to be used in DDBD for a given level of ductility and a hysteretic model. The flow diagram of the proposed method is shown in Figure 4-1.

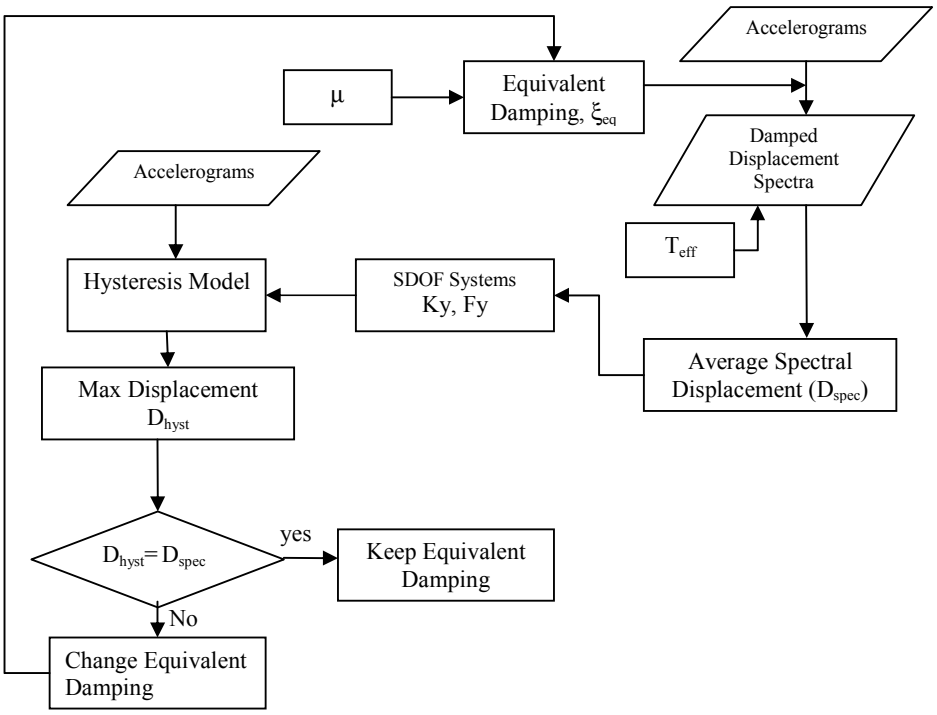

Figure 4-1 Flux diagram for the proposed methodology.

The process is repeated for effective periods from 0.5s to 4s each 0.5 s, for 5 ductility levels from 2 to 6. Six different hysteretic curves are used (section 5.2) and all the cases are analyzed for six records (chapter 5).

Step 1: Initially, an effective period (T_{eff}) and a ductility level (μ) are selected.

Step 2: Estimate the equivalent damping factor (ξ). For the first iteration this was based on Jacobsen's approach according to the hysteretic loop considered (Section 5.2). This equation was used only to have an initial estimate of the equivalent damping. However, after the results of the first iteration were obtained, the equivalent damping was changed in the next iterations to improve the substitute-structure/time-history agreement.

One important assumption used in this step and in the time-history analysis was the definition of the initial viscous damping factor (ξ_o). It was found that the initial elastic viscous damping would influence significantly in maximum response as explained section 7.2. In order to separate the influence of this factor from the hysteretic part of the problem, the initial elastic viscous damping factor was taken as zero in both design and time-history analysis.

Step 3: Determine the average damped displacement spectrum for the calculated value of ξ based on the average spectra obtained from the accelerograms described in section 5.

Step 4: An initial response displacement (Δ_{spec}) is obtained from the average damped spectrum for the selected effective period T_{eff} as shown in Figure 4-2.

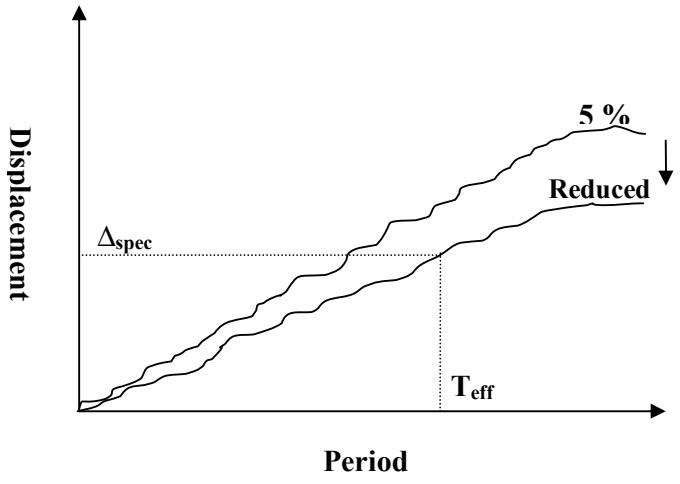

Figure 4-2. Selection of the displacement from the averaged reduced spectrum.

Step 5: For a given hysteretic model, the initial stiffness (K_{ini}) and yielding force (F_y). are defined using Δ_{spec}, mass (m_{eff}), effective period (T_{eff}) and the ductility (μ) as follows:

Yielding displacement

$$\Delta_y = \frac{\Delta_{spec}}{\mu} \quad \textbf{(4-1)}$$

Secant stiffness

$$K_e = 4\pi^2 m_{eff} / T_{eff}^2 \quad \textbf{(4-2)}$$

Maximum Force

$$F_{\max} = K_{eff} \Delta_{spec} \quad \textbf{(4-3)}$$

Depending if the envelope of the hysteretic model is bilinear or continuous (Figure 4-3) , it is possible to find the yielding force (F_y). The equations are given in section 5.2 for each hysteretic model. The initial stiffness can then be found from:

Initial stiffness

$$K_{ini} = \frac{F_y}{\Delta_Y} \quad \textbf{(4-4)}$$

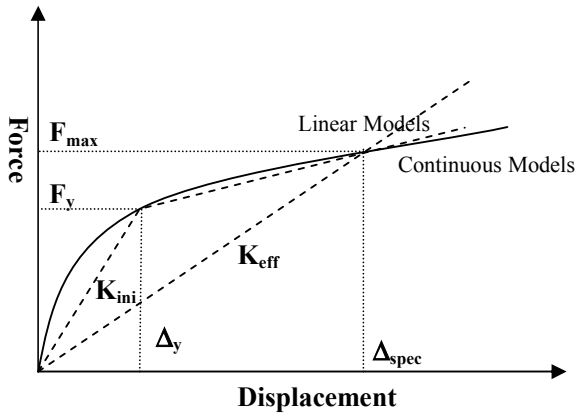

Figure 4-3 Characteristic values parameters of the SDOF system.

Step 6: Run time-history analysis for each of the records and obtain the maximum displacements.

Step 7: Compare the displacements obtained from step 6 with that from step 4. The values of the first and last iterations are stored. The first set of values is used to measure how accurately Jacobsen's equation can predict the viscous damping factor related to the design displacement (see results in chapter 0). The last set of values are use to check the convergence of the spectral and time-history displacements.

Step8: If the displacements are similar (within a tolerance of 3%) , keep the damping factor used and repeat the process from step 1 with a new T_{eff} and μ, otherwise, modify the damping factor and repeat the process from step 2.

5 ACCELEROGRAMS AND DISPLACEMENT SPECTRA

Six different synthetic accelerograms were selected in order to carry out the time-history analysis of the SDOF systems. All of them were constructed matching a given displacement design code shape response spectrum at 5% damping. The first accelerogram was a synthetic record developed by Bommer and Mendis [2004] for use specifically in this research. The rest of the accelerograms were artificial records obtained as part of this study and complemented with others obtained by Alvarez [2004] and Sullivan [2003]. All of these records were compatible with the ATC32 design spectrum for soil type C and PGA 0.7 g. [ATC32, 1996]. A brief description of the procedure and the tools used for both cases are given in the following sections.

5.1 BOMMER AND MENDIS

Mendis and Bommer selected several accelerograms from a world-wide records database in order to create code compatible response spectra. The target shape of the response spectrum was defined as described in section 5.1.1. From all the analyzed accelerograms, only one record could be matched to the spectrum for different levels of damping (see section 5.1.2). Regarding to this point, as explained in step 3 of the previous section, the inelastic displacement spectra are obtained from the elastic spectra using a reduction coefficient (η) [Borzi et al 2000]. This factor is analogous to the behaviour factor q used in force based design (Eq. (5-1)). The response spectra can be reduced according to the viscous damping factor using Eq. (5-2).

$$\eta = \frac{SD_{elastic}}{SD_{inelastic}} \tag{5-1}$$

$$\eta = \sqrt{\frac{2+\varepsilon}{7}} \tag{5-2}$$

This equation has demonstrated that the reduced spectra obtained match with good accuracy the median value of a set of accelerograms. However, there can be large variation when the spectrum of each accelerogram is reduced individually [Borzi et al, 2001]. In order to reduce this variation, the same authors that selected the accelerograms modified them using different techniques.

5.1.1 Target Design Spectrum

The target spectrum was obtained using the methodology proposed by Bommer et al [2000] for the scenario of stiff soil at 10 km from an earthquake of magnitude M_s 7.0. The peak ground motions are

obtained from the attenuation equations[1] of Tromans & Bommer [2002] using data from the European strong-motion data.

$$\log(PGA) = 2.138 + 0.214M_s - 1.049\log\sqrt{d^2 + 7.27^2} \qquad \text{PGA = 309.3 cm/s}^2\ (0.315g)$$

$$\log(PGV) = 0.141 + 0.356M_s - 1.058\log\sqrt{d^2 + 6.06^2} \qquad \text{PGV= 31.85 cm/s}$$

$$\log(PGD) = -1.995 + 0.597M_s - 1.144\log\sqrt{d^2 + 6.18^2} \qquad \text{PGD = 9.11 cm}$$

The parameters and the procedure used in the methodology used by Bommer are described briefly afterwards.

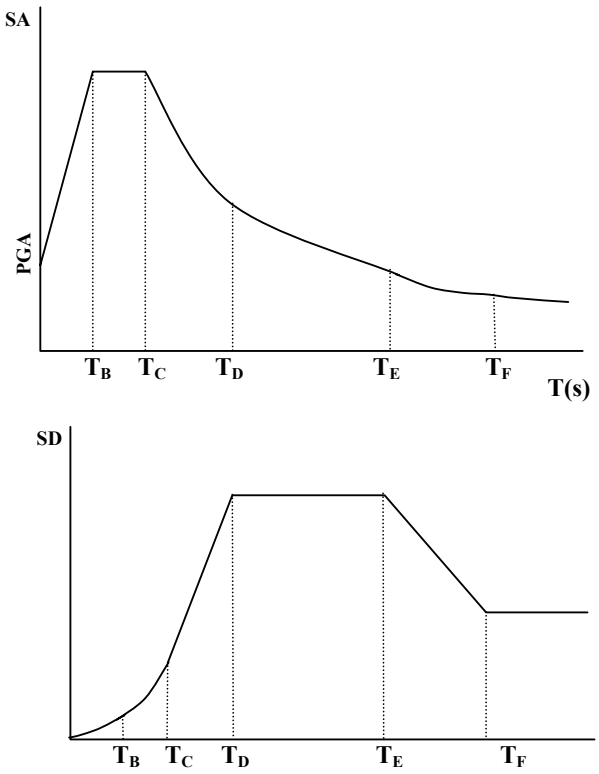

Figure 5-1 Compatible acceleration and displacement spectrum as defined by Bommer *et al.* (2000) [from Bommer,2004].

The corner periods, T_C and T_D, are defined by equations:

$$T_C = 5\left(\frac{PGV}{PGA}\right) = 0.515 \text{ s}$$

$$T_D = 8\left(\frac{PGD}{PGV}\right) = 2.288 \text{ s}$$

[1] Unit in cm and seconds

The displacement plateau is defined by the following equation:

$$SD = \frac{PGA(2.5\eta)(T_C T_D)}{4\pi^2} = \quad 23.08 \text{ cm} \qquad \text{(for 5\% of damping)}$$

where η is the scaling factor for damping levels mentioned previously, taking a value of unity for 5% of critical damping. The adjustment for other levels of damping is made using a similar type of equation as Eq. (5-2) but with different coefficients (10 instead of 7 and 5 instead of 2), proposed by Bommer *et al*. [2000] which is included in the current version of EC8. The obtained target spectrum for different damping levels is shown in Figure 5-2. However, the adjusted records, match better to the damped design spectra using the initial coefficients of Eq. (5-2).

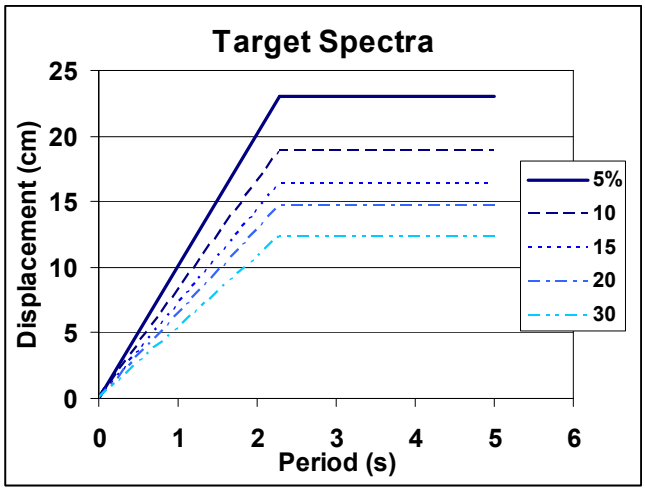

Figure 5-2 Target spectrum.

5.1.2 Records (Manjil, Iran, 20th June 1990)

As mentioned previously, only the record of Manjil matched the spectral shape after the process. The original accelerogram is the longitudinal component of the M_s 7.3 Manjil earthquake, in the Ghazvin station which is located in stiff soil at a distance of 51 km from the fault rupture. The first step was to scale the record by a factor of 2.07 in order to produce a better match with the displacement spectra (Figure 5-3).

5.1.3 Spectral Matching

In order to improve the match of the selected accelerogram with the target spectra, Mendis and Bommer carried out an adjustment using wavelets. They used the program RSPMATCH, developed by Dr Norman A. Abrahamson [1998]. Consulting with the developer, they fount that the program is currently only able to provide reasonable matches to two different damping levels in the current version of the program. The investigation carried out by these two authors confirmed the tendency of the program to produce highly unstable results if more than two target spectra are used.

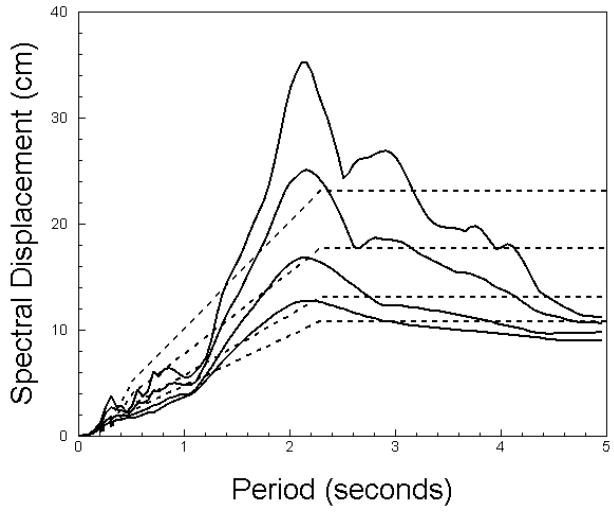

Figure 5-3 Displacement spectra from the scaled Manjil record (solid lines) and the design spectra (dashed lines) (5, 10, 20 and 30% damping) [from Bommer,2004].

The spectral matching is performed in the time domain, using the acceleration spectra as the target, but the results are presented here in terms of displacements. Finally, the match of the record was made for 10% and 20% and 30% viscous damping factor (Figure 5-4).

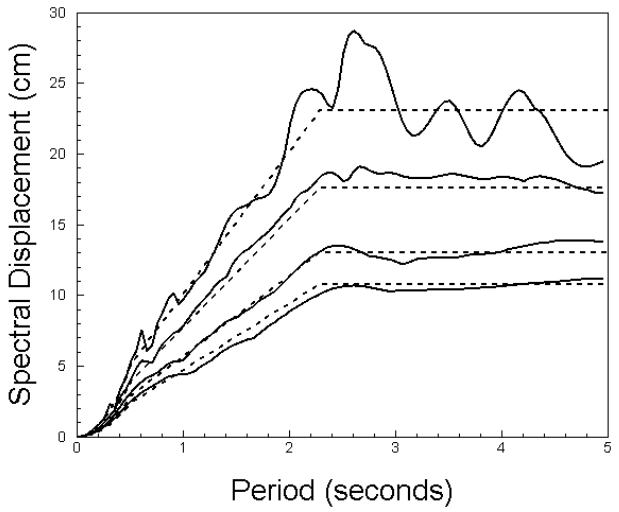

Figure 5-4 Displacement spectra from the adjusted Manjil record (solid lines) and the design spectra (dashed lines). (5, 10, 20 and 30% damping) [from Bommer,2004].

5.1.4 Adjusted Accelerogram

The adjusted accelerograms present some differences with the original record (Figure 5-5), given than the wavelets modify the original signal producing an artificial accelerogram. However, the signal obtained retains the physical characteristics of the original record in the time domain.

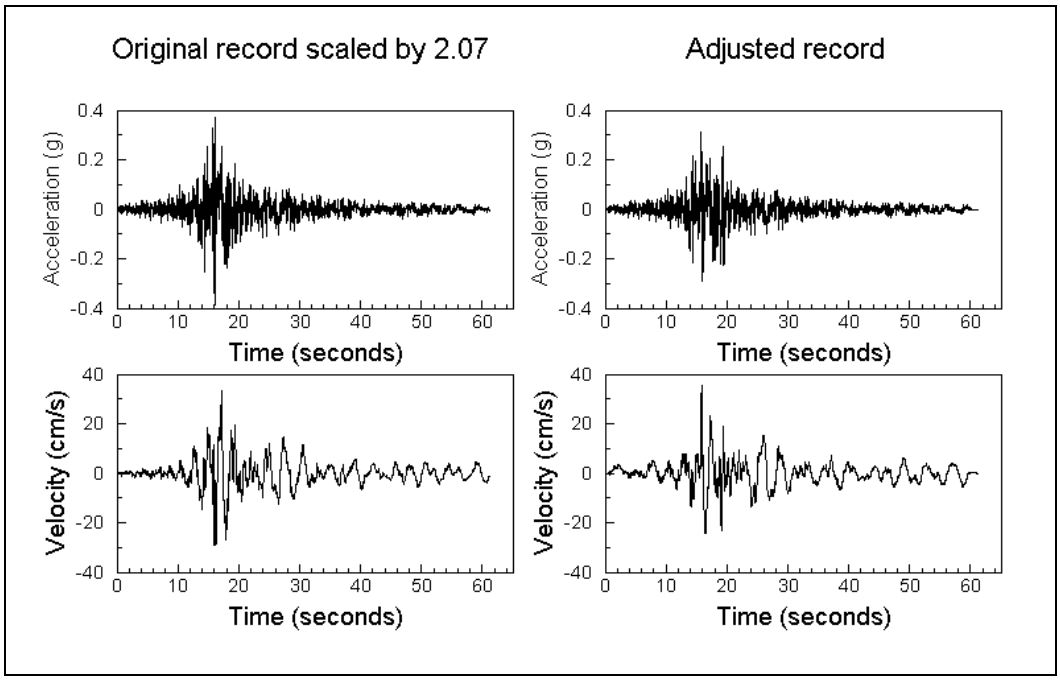

Figure 5-5 Acceleration and velocity time-histories of the scaled (*left*) and adjusted (*right*) accelerograms [from Bommer,2004].

For the scope of the study, it was desirable to have a corner period at 4 s. Therefore the scale of time of the accelerograms was modified by increasing the duration of the accelerograms taking step increments of half the original time step. The displacement spectra for this modified record is shown in Figure 5-6.

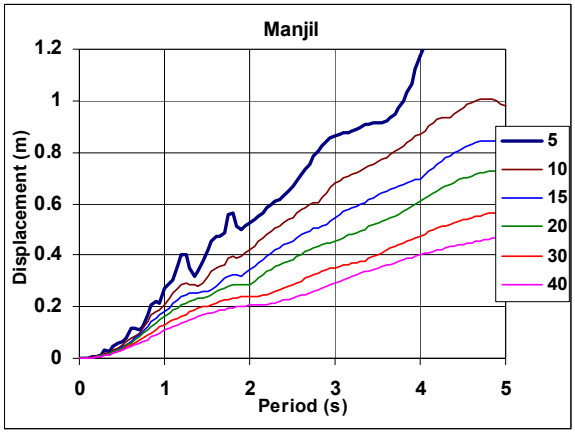

Figure 5-6 Modified Manjil record response spectra.

5.2 ARTIFICIAL ACCELEROGRAMS

In order to have additional data which could allow observing a particular trend of the results, five additional accelerograms were selected from a set of artificial records obtained for this study complemented by a set prepared beforehand by Alvarez [2004] and Sullivan [2003].

The target design spectrum for this set of accelerograms was the one proposed by Caltrans (Figure 5-7) for a soil type C and PGA of 0.7 g. For these accelerograms, it was not necessary to obtain an initial record but they were obtained from a random process carried out by the specific software called "SIMQKE"[Carr, 2002].

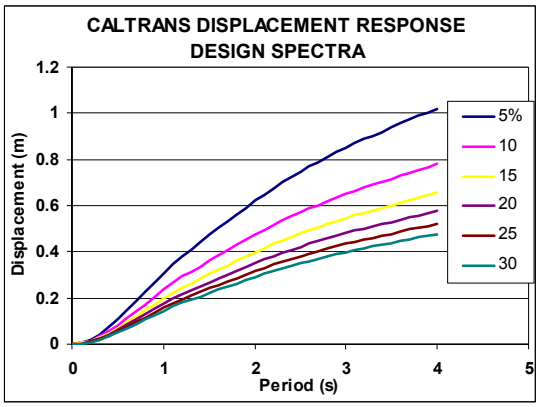

Figure 5-7 Caltrans Target Displacement Design Spectrum for soil type C (PGA= 0.7 g).

The reduced displacement response spectra for different levels of damping for this plot were also obtained using Eq. (5-2). The match of these reduced spectra is better using this equation that the one proposed by EC8. However, the reduced displacement spectra of the artificial spectra obtained with SIMQKE were computed using the program SPECTRA [Carr, 2002].

It was necessary to carry out several attempts before obtaining several accelerograms that would adjust the design spectrum within an acceptable margin. Finally, five accelerograms were selected from the generated set of artificial records; Figure 5-8 shows the response spectra for different levels of damping for the selected accelerograms.

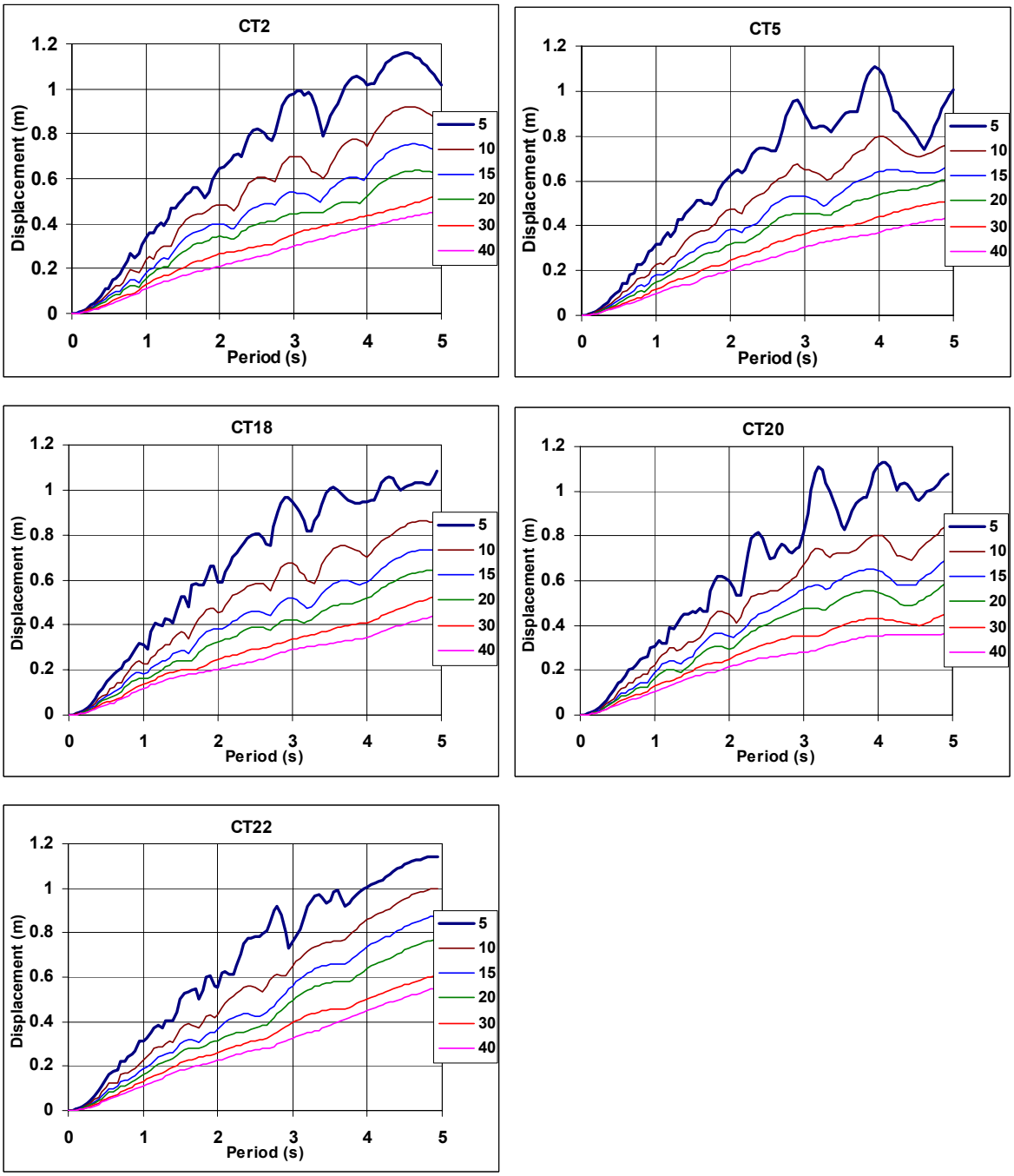

Figure 5-8 Displacement Response Spectra for the adjusted records

The average displacement response spectra used for the design step described in the methodology is shown in Figure 5-9. As observed, this average spectra have approximately smooth shapes and have good approximation to the target Caltrans spectra.

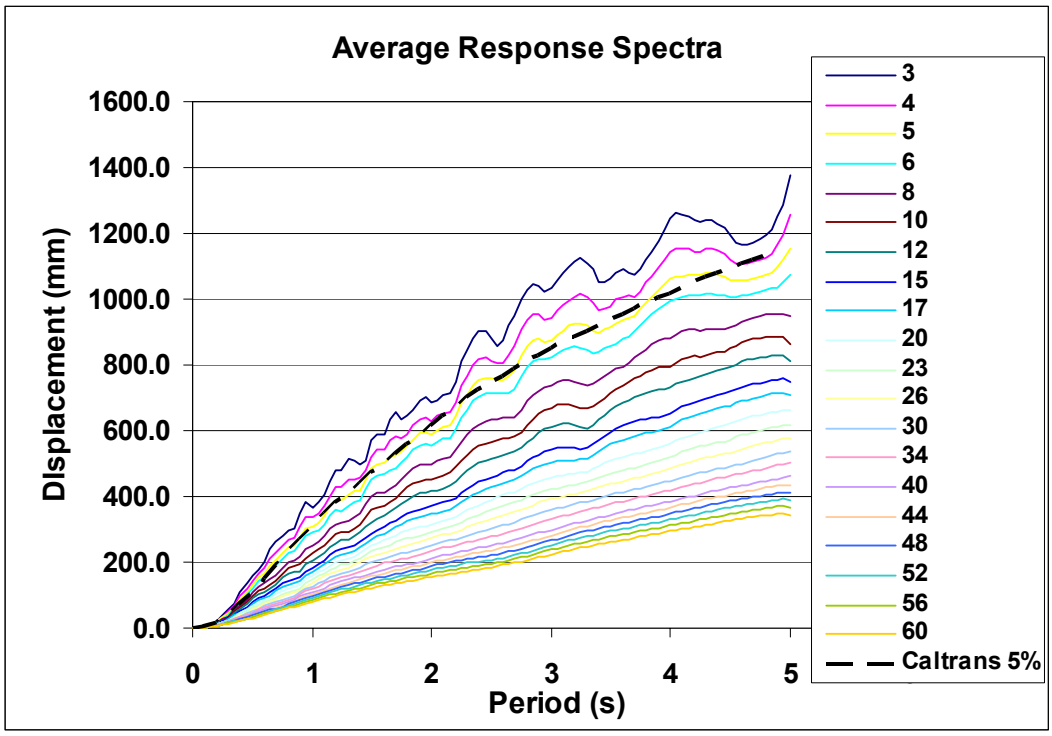

Figure 5-9 Average displacement response spectra

6 HYSTERETIC RULES

The assumptions which form the basis of the current equations used to estimate the equivalent viscous damping factor were discussed in chapter 3. It was seen that Jacobsen's approach equates the area inside complete closed loops of a viscous damper and a hysteretic loop. However, few equations have been defined for specific hysteretic loops. In order to observe the behaviour of the equivalent viscous damping factor several hysteretic rules were used in the analysis. Additionally, for the same hysteretic loop some parameters were changed to increase the range of possibilities of the response. This is justified by the fact that the response using the same hysteretic loops but with different parameter may vary significantly.

Six hysteretic models were used in the analysis: Elastic perfectly plastic (EPP), Bilinear type, a "narrow" and a "fat" Takeda loop, a Ramberg Osgood model and finally a ring spring (flag shape) model. A brief description of the hysteretic rules is shown in the next sections.

6.1 TAKEDA

This model is used to represent the non-linear behaviour of concrete structures and members (Figure 6-1). There are three factors that define the fatness of the loops; post yielding stiffness (r), unloading stiffness parameter (α) and reloading stiffness parameter (β). Two variations of this model were used for the analysis; one representing systems with narrow loops ($\alpha = 0.5$ and $\beta = 0.0$) such us walls or columns and other with fatter loops ($\alpha = 0.3$ and $\beta = 0.6$) such as beams. Post yielding stiffness factor was kept constant for the two models (r =0.05). The theoretical equivalent viscous damping for the Takeda model depends on these factors. Equation (6-1) is the equivalent viscous damping obtained from the Jacobsen approach [Kowalsky and Ayers,2000]

$$\xi_{equ} = \frac{2}{\pi}\left\{1-\frac{3}{4}\mu^{\alpha-1}-\frac{1}{4}\left[\frac{r\beta\mu}{\gamma}\left(1-\frac{1}{\mu}\right)+1\right]\left[2-\beta\cdot\left(1-\frac{1}{\mu}\right)-\mu^{\alpha-1}\gamma\right]-\frac{1}{4}\left[\frac{r\beta^2\mu}{\gamma}\left(1-\frac{1}{\mu}\right)^2\right]\right\} \qquad \textbf{(6-1)}$$

$$\gamma = r\mu - r + 1$$

$$k_u = k_o\left(\frac{d_y}{d_m}\right)^{\alpha} \quad \text{Unloading stiffness (see Figure 6-1)} \qquad \textbf{(6-2)}$$

where r is the post-yielding stiffness ratio, m is the displacement ductility, a is the unloading stiffness parameter and b is the reloading stiffness parameter. Two versions were used in the

analyses. The fatness of the loop is controlled by the factors α and β. The former parameter controls the slope of the unloading stiffness; as this parameter increases the loop tend to be fatter. The maximum value of this parameter is 1, in which case the unloading and loading stiffness are equal. A value of 0.5 is considered to be the lowest value of this parameter, according to experimental observations. The parameter β defines the point where the reloading curve reaches the post elastic branch. Values between 0.6 (fat loop) and 0 (narrow loop) are considered to be the extreme of the variation range.

For this project a "thin" Takeda model with α= 0.5 and β=0 was considered appropriated for bridge piers and wall structures. The second "fat" Takeda model (α=0.3, β=0.6) was intended to be appropriate for reinforced concrete frames. In both cases the post-yield stiffness ratio was taken as 0.05.

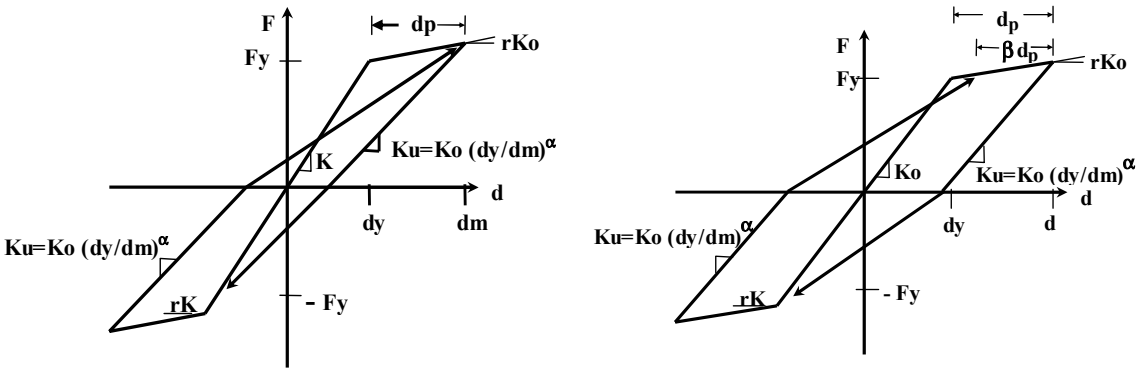

Figure 6-1 Takeda Model. [from Ayers, 2000]

Figure 6-2 illustrates the EVDF for four different Takeda models described in Table 6-1. The EVDF increases as β increases and *r* and α decreases.

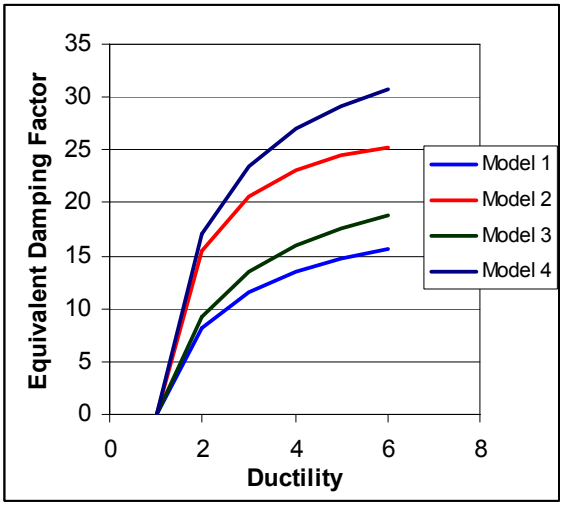

Figure 6-2 equivalent viscous damping factor for Takeda models

Table 6-1. Takeda models

Model	α	β	*r*
Model 1	0.5	0	0.05
Model 2	0.3	0.6	0.05
Model 3	0.5	0	0
Model 4	0.3	0.6	0

6.2 ELASTO PLASTIC RULE (EPP)

The EPP model was included solely because of its historic importance in seismic time-history analysis. Its closest approximation in real structures is a flexible structure isolated with a flat coulomb (friction) damper. However, the loops tend to overestimate the amount of energy dissipated in most structural systems. The rules of this model are very simple and consist of a loading and unloading stiffness (K_o) that changes when the yielding force (F_y) has been reached. After yielding, the stiffness drops to 0 if the system has not hardening (Figure 6-3).

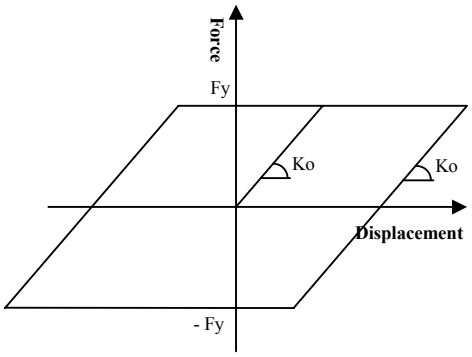

Figure 6-3 Elastic Perfectly plastic Hysteretic Loops. (No Hardening)

The theoretical equivalent damping for this hysteresis rule is significantly large given the area enclosed by the loops in proportion with the elastic stored energy, and is given by Eq. (6-3).

$$\varepsilon_{equ} = \frac{2}{\pi}\left[\frac{(1-r)(u-1)}{\mu - r\mu + r\mu^2}\right] \qquad \textbf{(6-3)}$$

where r is the post yielding stiffness coefficient and α is the unloading degrading coefficient as defined in Eq. (6-2). For the case of the elastic perfectly plastic model with no post yielding stiffness and no unloading stiffness degradation Eq. (6-3) simplifies to Eq. (6-4)

$$\xi_{equ} = \frac{2(\mu - 1)}{\pi \cdot \mu} \qquad \textbf{(6-4)}$$

6.3 BILINEAR

This hysteretic model was intended to model the dynamic behaviour of a structure incorporating an isolation device (friction pendulum system FPS). This mechanism combines a sliding action and a restoring force by geometry [Naeim and Kelly, 1999]. Due to the properties of the dissipating system, the initial stiffness is very high so in Figure 6-4 the loop starts directly from zero displacement and the characteristic strength. However, when combined with the structural flexibility, the FPS is modelled with a bilinear envelope (Dash line). The equivalent damping is given by Eq. (6-5).

$$\xi_{equ} = \frac{2(\mu - 1)}{\pi\mu(1 + r(\mu - 1))} \quad \textbf{(6-5)}$$

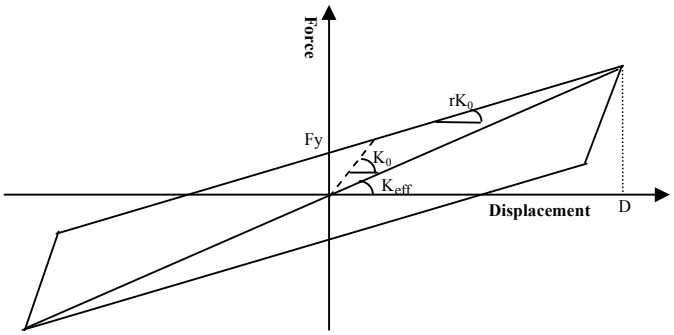

Figure 6-4 FPS hysteretic loop.

In general, the FPS devices are used to isolate the movement of the superstructure of bridges from that from the piers. Therefore, the hysteretic model should represent the combination of the force deformation relationship of the piers and the FPS device. Given that there are many possible combinations that can be considered the values of initial stiffness and post yielding stiffness were selected based in some assumptions that are typical in design.

The main assumptions are that the response of the pier is always linear with a fundamental period (T_p) of 2 seconds. The period of the FPS (T_{FPS}, based on rK_0) is equal to 4s. Finally, r = 1/50. With these assumptions, the system (pier-FPS) is modelled as a bilinear system with a post yielding coefficient of 0.2. (Assuming a weight (w)=10.000 KN).

Pier linear stiffness $K_p = 4\pi^2 \frac{m}{T_p}$ = 10.07 N/mm

FPS stiffness $K_{FPS} = rK_o = 4\pi^2 \frac{m}{T_{FPS}}$ = 2.52 N/mm

FPS initial stiffness $K_0 = \frac{1}{r} K_{FPS}$ = 125.9 N/mm

System's initial stiffness $\frac{1}{K_e} = \frac{1}{K_p} + \frac{1}{K_o}$ K_e = 9.33 N/mm

System's post-elastic stiffness $\frac{1}{K_r} = \frac{1}{K_p} + \frac{1}{K_{FPS}}$ K_r = 2.01 N/mm

Systems post yielding stiffness coefficient (K_r / K_e) = 0.22

6.4 RAMBERG OSGOOD

This model is often used to describe the resistance deformation strain relation of steel members in frame analysis. The loading curve is defined by Eq. (6-6):

$$\frac{D}{D_y} = \frac{F}{F_y}\left(1 + \left|\frac{F}{F_y}\right|^{\gamma-1}\right) \tag{6-6}$$

The curve passes at (Fy, (2Dy)) for any value of γ, which controls the shape of the primary curve. As shown in Figure 6-5, the loading curve may vary from a linear elastic line for γ = 1.0, to an elasto-plastic bilinear segment, for γ = ∞.

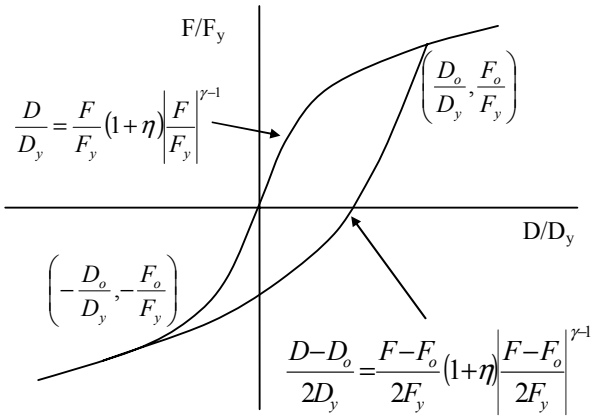

Figure 6-5 Ramberg Osgood curve. From [Otani,1981]

The unloading curve from the maximum point (Do, Fo) follows the equation:

$$\frac{D - D_o}{2 \cdot D_y} = \frac{F - F_o}{2 \cdot F_y}\left(1 + \left|\frac{F - F_o}{2 \cdot F_y}\right|^{\gamma-1}\right) \tag{6-7}$$

The force is computed by an iterative procedure using the Newton – Rapson method. As pointed out by Otani [1981] this hysteretic model dissipates energy even if the ductility factor is less than one, the dissipated energy is sensitive to γ, increasing with the increasing of this parameter.

There are four input parameters which define the hysteretic models: the yield strength (F_y), yield displacement (Dy), Ramber Osgood Parameter (γ), and the convergence limit for the Newton Rapson procedure (β_1). The EVDF of the Ramberg Osgood model depends on the value of γ and increases as the value of this parameter increases as described in Eq. (6-8). This parameter was selected as being reasonably appropriate for structural steel members equal to 7.

$$\xi_{equ} = \frac{1}{\pi}\left(1 - \frac{2}{\gamma + 1}\right) \cdot \left(1 - \frac{1}{\mu} \cdot \frac{F}{F_y}\right) \tag{6-8}$$

6.5 RING SPRING MODEL (FLAG SHAPE)

This model was original developed to model a specific kind of energy dissipation [Hill 1994], however, it can be also used to model prestressed concrete (post tensioned unbonded concrete). The model is characterized by small energy dissipation given the small enclosed areas in the loop, and also by the absence of permanent deformation given that the curve always return to the origin (Figure 6-6).

The model is described by the initial stiffness (K_0), the post elastic coefficient (r), the unloading steep stiffness coeffiecient (r_{steep}), the unloading lower stiffness coefficient (r_{lower}) and a dummy displacement d_{xinit}. The yielding force (F_y), yielding displacement (d_y), and the point where the unloading branch intersects the initial loading branch (d_0,F_0) rest of the parameters can be obtained from Eq. (6-9a)

$$d_o = r_{lower} d_{x\,init} \tag{6-9a}$$

$$d_y = \frac{r(1-r_{lower})}{1-r} d_{x\,init} \tag{6-9b}$$

$$F_y = k_0 d_y \tag{6-9c}$$

$$F_0 = k_0 d_0 \tag{6-9d}$$

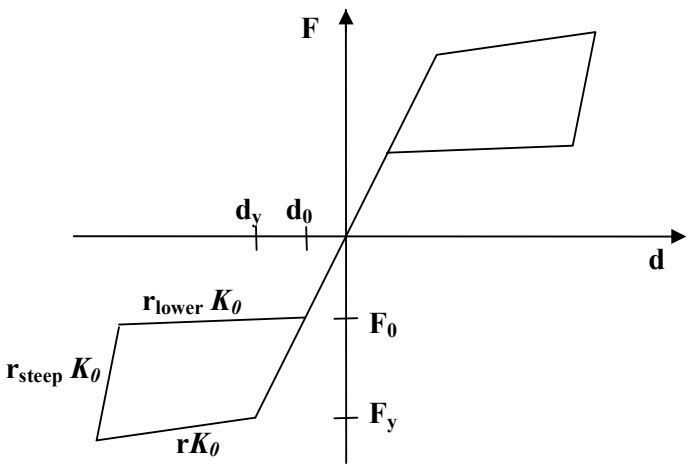

Figure 6-6 Ring spring model [Hill, 1994], from Carr [2002].

The expression obtained using Jacobsen's approach to estimate the EVDF for this hysteretic rule is significantly complicated and extended, so it will not be included here. However, Figure 6-7 shows the EVDF for all the hysteretic model described in this chapter for the parameters specified in Table 6-2..

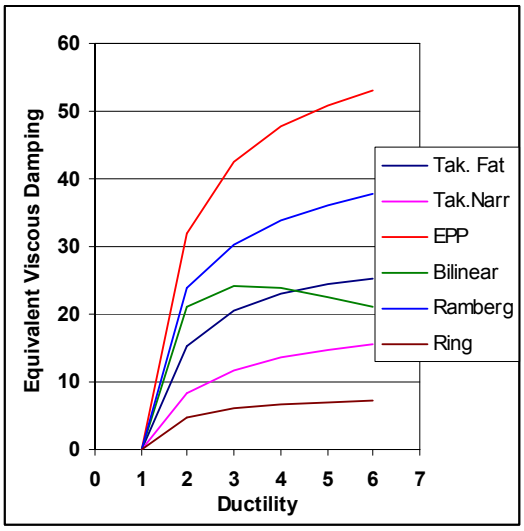

Figure 6-7 EVDF for the selected hysteretic models

Table 6-2. Model Parameters

Model	Parameters
Takeda Fat	r=0.05 α= 0.3 β=0.6
Takeda Narrow	r=0.05 α= 0.5 β=0.0
EPP	r=0.0
Bilinear	r=0.2
Ramberg	γ=7
Ring Sring	r_{lower}=0.035, r_{steep}=1,r=0.04

7 MODELLING ASSUMPTIONS AND RESULTS

7.1 INTRODUCTION

Time-history analysis were carried out using the program RUAUMOKO [2003], using a Newmark constant average acceleration integration scheme with $\beta = 0.25$. As described in chapter 4, this procedure was carried out iteratively until the displacement of the equivalent SDOF system is the same for the time-history and for the design spectral analysis. Time step used for the integration was taken as half of the discretization step of each accelerograms, this is, 0.005 s except for Manjil adjusted record which has a discretization step of 0.0045.

The results shown in this chapter are the average of the individual analysis for each of the six accelerograms used for each hysteretic model. The C.O.V for each case are also included in order to observe the variability of the results. Three set of plots are analysed for each case; the first one consist on the ratio between the displacements obtained from the time-history analysis (THA) and those from spectral design procedure (using DDBD for the equivalent damping from Jacobsen's approach). From this ratio would be possible to estimate how accurate is the Jacobsen's approach to estimate the maximum time-history displacements (effective displacements).

Second set of plots show the effective equivalent viscous damping factor obtained from the iterative procedure. Finally, the last set of plots show the dispersion in terms of C.O.V of the effective EVDF.

7.2 INITIAL VISCOUS DAMPING

The initial elastic viscous damping used for time-history analysis of SDOF systems has been traditionally defined in practice by use of a constant damping coefficient corresponding to 5% of critical damping though lower values are sometimes used for steel structures. This value is assumed to represent the different sources of energy dissipation when the structure is considered in the elastic range. It is not clear that constant coefficient damping is appropriate for structures responding inelastically, since the hysteretic models generally incorporate the full structural energy dissipation in the inelastic range, and other contributory mechanism, such as foundation damping will be greatly reduced when the structure enters the inelastic range. It would appear that tangent-stiffness proportional damping would be more appropriate than constant coefficient (initial-stiffness proportional, or mass-proportional) damping in modelling initial elastic damping in seismic response. The adoption of different characteristic stiffnesses in DDBD (secant stiffness) and time-history analyses (initial stiffness) further confuses the issue. From

analyses conducted parallel to this study [Priestley and Grant, 2005], it was found that the choice of damping model used to represent elastic damping has a significant effect on the response of the system. As the results of Priestley and Grant's study were not available at the start of the present study, and in order to eliminate the effects of this uncertainty and clarify the effective damping due only to hysteretic behaviour, the initial viscous damping was taken as zero in both the DDBD process, and the time-history analyses

7.3 TAKEDA

7.3.1 Model 1 (Narrow type)

The results of the time-history analysis (THA) / initial design displacement ratio presented in Figure 7-1 indicate that displacements for short periods (less than 1s) are overestimated indicating a conservative design; meanwhile, for larger periods the average displacements obtained by the THA are larger than the initial design displacements (using EVDF given by Jacobsen's approach Eq. (6-1)). This means that the effective displacements are underestimated, indicating an unconservative design. However, the initial design displacements are in general inside ± 10% the value estimated by the THA with a coefficient of variation (C.O.V) around 0.15, which is an acceptable range for design. A slight correction of the damping estimated using Jacobsen's approach would improve the results.

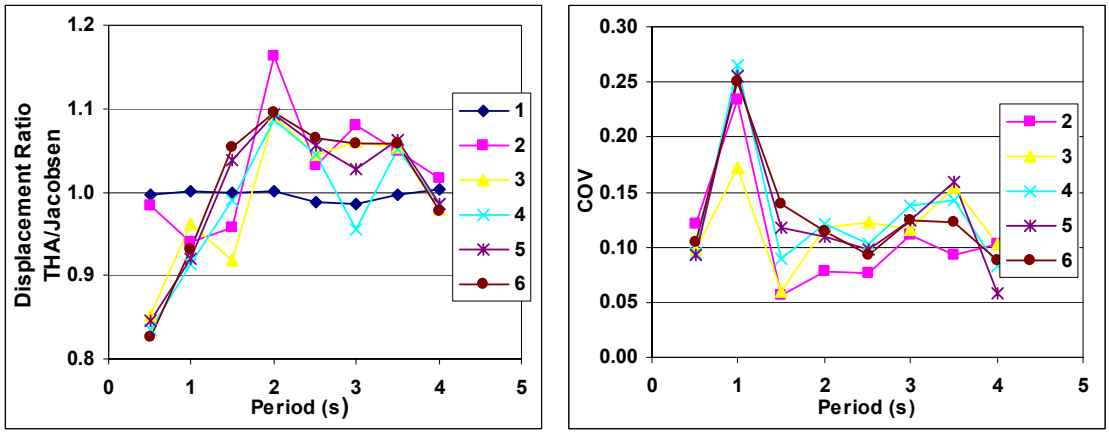

Series represent ductility level from 1 to 6

Figure 7-1 Time-history analysis / Initial design displacement average ratio (left) and dispersion (right) for Takeda model (Narrow type, $\alpha = 0.5$, $\beta = 0.0$, r=0.05), based on Jacobsen's Approach.

The lack of consistency in matching the design and time-history displacement justifies the application of the procedure described in chapter 4. The steps described there were applied for all the six synthetic accelerograms. Figure 7-2 shows the average results (six records) of the equivalent damping factor obtained after the iterative procedure. Using the EVDF shown in the figure, it is possible to obtain approximately the same displacement from a design displacement spectra and a non-linear time-history analysis (for an effective period and a given level of ductility).

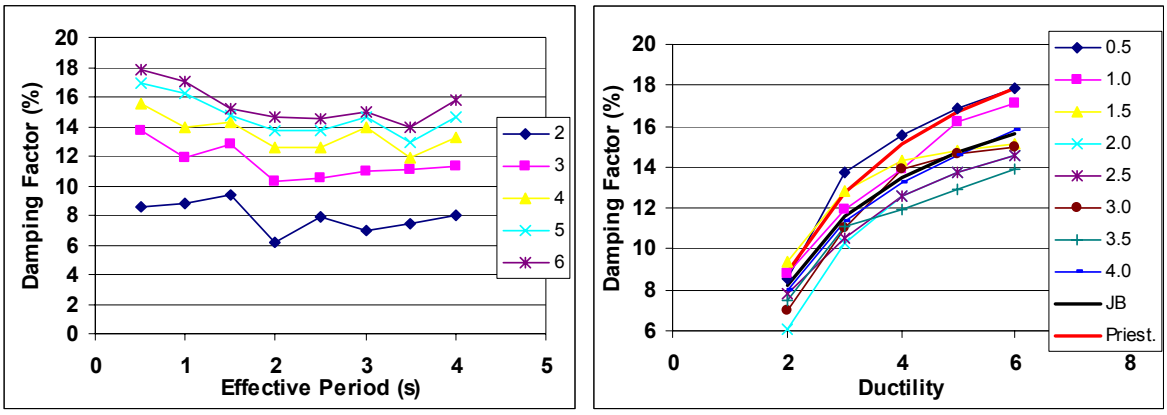

Series represent ductility level from 2 to 6 *Series represent periods from 0.5 to 4.*

Figure 7-2 Average Equivalent Damping for Takeda model (Narrow type, $\alpha = 0.5$ and $\beta = 0.0$)

Figure 7-2 (left) shows that there is a slight dependency of the EVDF on the period but the dependency on ductility (right) is much stronger. In the left plot (EVDF vs Ductility) the bold black line (JB) represents the estimation of the damping obtained using Jacobsen's approach. It can be observed that this estimation gives an approximate average of the EVDF for all periods and gives a good representation of the damping variation with ductility. The red bold line gives the estimation of the same factor using Eq. (3-16a) proposed by Priestley. This equation gives a larger estimation of the EVDF because it does not take into account the value of the post elastic coefficient (*r*). In general, there is a gradual decrease of the damping from the short periods to the intermediate periods until a constant value is reached. The same pattern occurs for different levels of ductility, being more irregular at lower ductility levels.

The coefficient of variation associated to the average damping ranges between 0.1 to 0.25 (Figure 7-3); however it would be necessary to carry out more analysis with additional records in order to obtain a reliable value of the coefficient of variation. From the available results it is possible to observe that the coefficient does not follow any particular trend either in terms of period or in terms of ductility. It would be possible then to select a constant conservative value average value of this coefficient, which could be approximately 0.2.

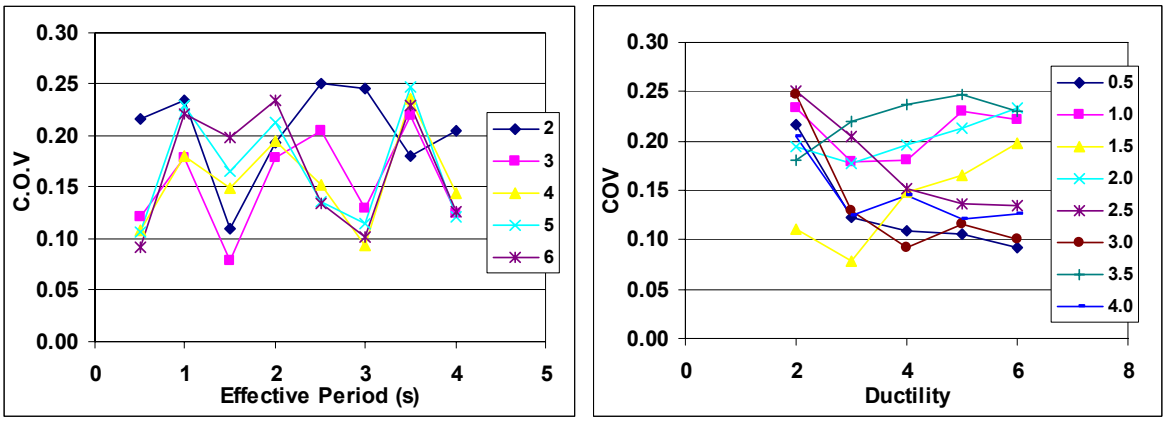

Series represent ductility level from 2 to 6 *Series represent periods from 0.5 to 4.*

Figure 7-3 COV of the effective EVDF for Takeda Model (Narrow type, $\alpha = 0.5$ and $\beta = 0.0$).

7.3.2 Model 2 (Fat Type)

The EVDF estimated by Jacobsen's approach is given by Eq. (6-1) with a different set of coefficients. The theoretical energy dissipation is larger than in the previous case. As shown in Figure 7-4, the displacements obtained from THA are in general larger than the initial design displacements. There is a slight tendency to estimate better the displacements for short periods than for large periods. However the trend is not very clear for all ductility levels. In terms of dispersion, the C.O.V seems not to have any relationship with ductility nor period, even if there is a large reduction of the C.O.V for intermediate periods. In practical terms the C.O.V for the results is around 0.2. It is clearly seen that Jacobsen's approach need a calibration for this rule, given the significant underestimation of the effective displacements.

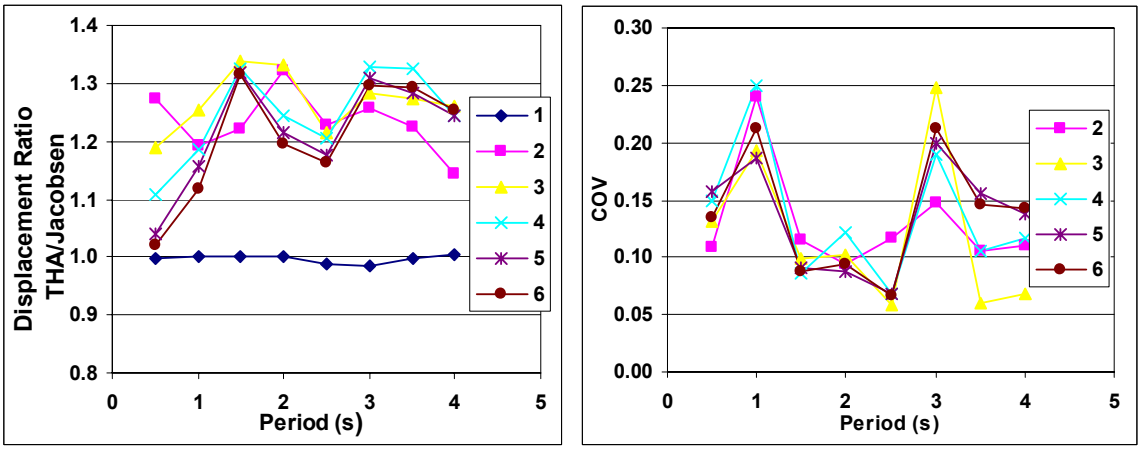

Series represent ductility level from 1 to 6

Figure 7-4 Time-history analysis / Initial design displacement average ratio (left) and dispersion (right) for Takeda model (Fat type, $\alpha = 0.3$ and $\beta = 0.6$, r=0.05), based on Jacobsen's Approach.

The results of the iterative procedure are shown in Figure 7-5. The obtained effective damping shows the same trend as the narrow Takeda model. In general, there is a decrease of the damping from the short

periods to intermediate periods until an approximate constant damping is reached. The damping given from Jacoben's (JB) approach in Eq. (6-1) is overestimated, which is the reason why the average THA/ initial design displacement ratio is, in general, significantly larger than 1. The Jacobsen's equation however, gets more or less the right pattern of dependency on ductility. Equation (3-16a) proposed by Priestley (red line) gives a better match to the effective damping. However it still overestimates this factor for some periods.

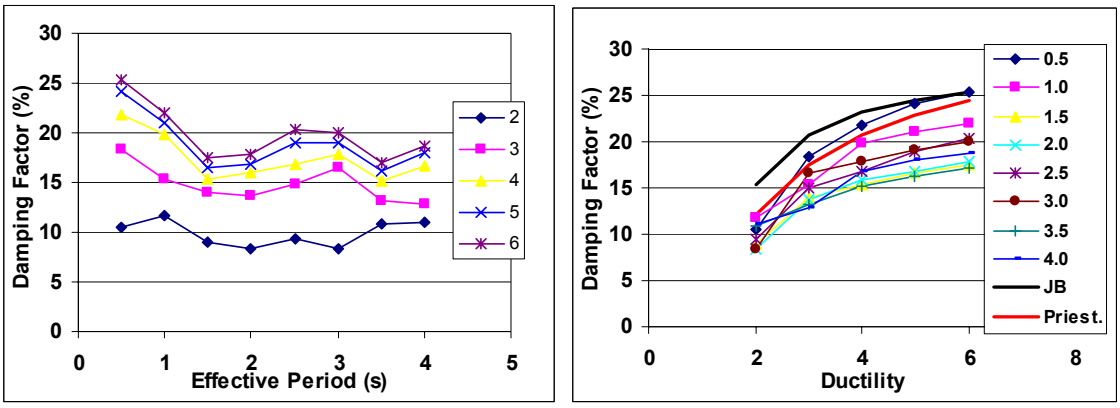

Series represent ductility level from 2 to 6 *Series represent periods from 0.5 to 4.*

Figure 7-5 Average Equivalent Damping for Takeda model (Fat type, $\alpha = 0.3$ and $\beta = 0.6$)

For this hysteretic rule, the dispersion of the data, expressed with the coefficient of variation (COV) tends to be larger than in the case of the "narrow type" Takeda model, but in practical terms there seems to be almost no difference (Figure 7-6), therefore, a C.O.V of 0.20 could be taken to define the dispersion of the EVDF.

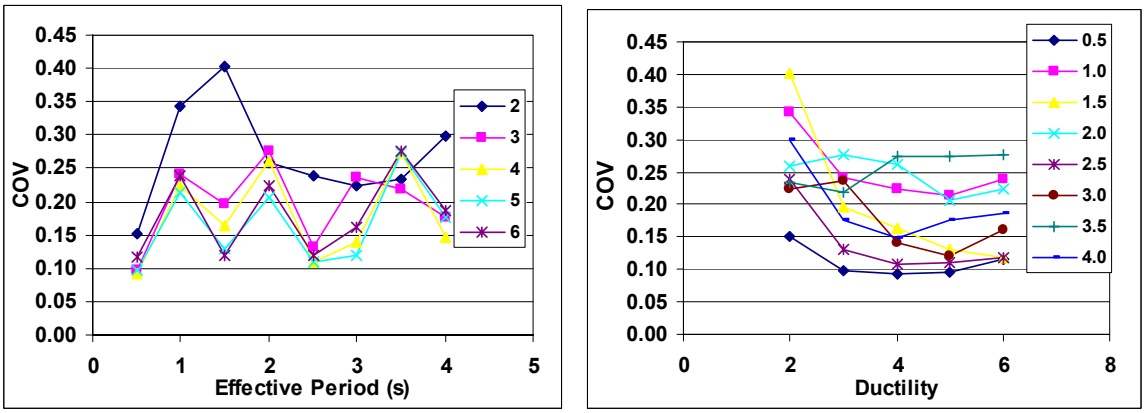

Series represent ductility level from 2 to 6 *Series represent periods from 0.5 to 4.*

Figure 7-6 COV of EVDF for Takeda Model (Fat type, $\alpha = 0.3$ and $\beta = 0.6$).

7.4 BILINEAR

For this type of hysteretic model, the design displacements using damping from Eq. (6-3) are significantly underestimated for most cases. Figure 7-7 shows that for short periods the average displacement can be

predicted safely with an acceptable level of accuracy except for high ductility levels (5 and 6). For the rest of the cases, the results are unconservative tending to be even more unsafely as ductility decreases. The dispersion of the displacement ratio is lower than in the previous two cases, showing more stability of the response. From these plots, it is demonstrated that Jacobsen's equation needs further corrections.

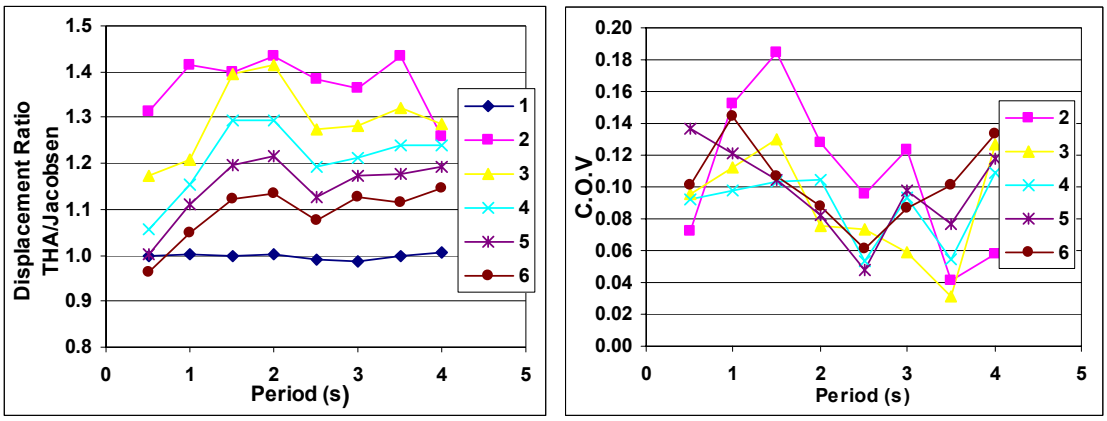

Series represent ductility level from 1 to 6

Figure 7-7Average displacement for the bilinear hysteresis model (Jacobsen's approach)

The effective damping follows the same pattern as in the previous model; reducing as period increases until a constant damping is obtained (Figure 7-8). The variation is also stronger in terms of ductility than in terms of period. Jacobsen's equation (Eq.(6-3)- black line), overestimates in general, the effective EVDF; Additionally, in this model, the variation with ductility is not well represented. The real data tends to follow a pattern that could be described better for a curve that is always increasing with the square root of the ductility as in the EPP or Takeda models. This behaviour indicates that Eq. (6-4) is not reliable in terms of variation with ductility, as the post elastic stiffness coefficient (r) increases.

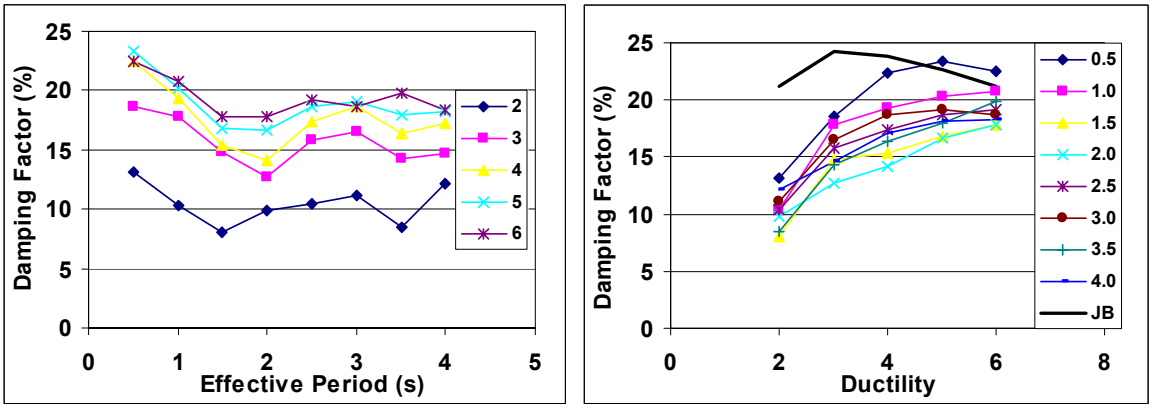

Series represent ductility level from 2 to 6

Series represent periods from 0.5 to 4.

Figure 7-8 Equivalent Viscous Damping Factor for bilinear hysteretic loop (K_1=0.2K_0)

The variation associated with the average value of the EVDF for the bilinear hysteretic model does not seem to have a clear dependency on period nor ductility. Figure 7-9 shows a larger and more unstable C.O.V of the EVDF as ductility decreases but without any specific tendency. In this model, the C.O.V

could also be taken as 0.2 for all periods and ductility levels. The large C.O.V presented for a ductility of 2 are caused by a particular record. However, it would be expected that as the number and the quality of the records increase, this peak would tend to disappear.

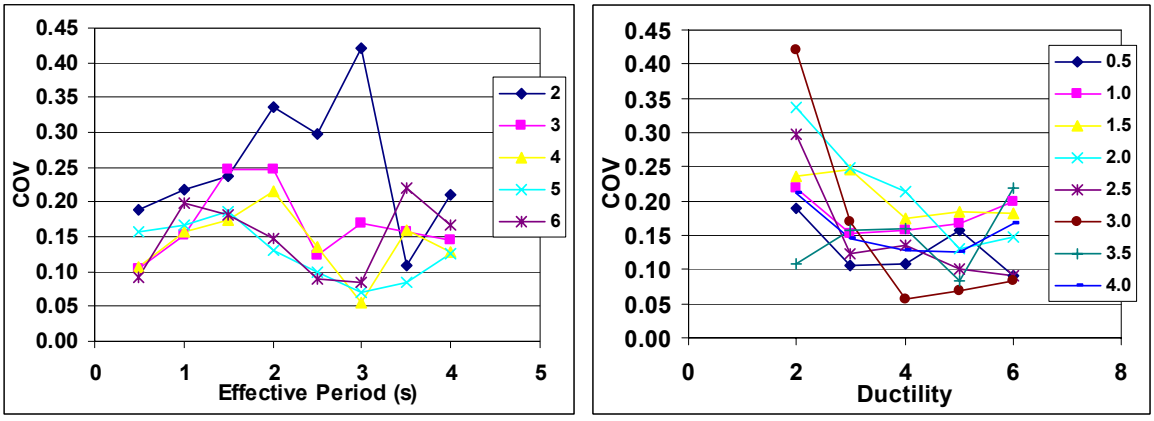

Series represent ductility level from 2 to 6 *Series represent periods from 0.5 to 4.*

Figure 7-9 COV of EVDF for FPS Model

7.5 ELASTIC PERFECTLY PLASTIC RULE (EPP)

The average ratio between the time-history design and design displacements for the EPP hysteretic model indicates that there is a significant overestimation of the effective damping (Figure 7-10). Therefore, Jacobsen's equation Eq. (6-4) needs adjustment This hysteretic rule is the one with the largest displacement ratio in comparison with the other hysteretic models analyzed. Additionally to the THA/Initial design displacement ratio which indicates displacements more than twice the design displacement, the variability of the response is vary large. This indicates that the response is unstable, which can be attributed in part to the post yielding coefficient used (r=0). Based on this result, the displacement obtained using this type of model, using Jacobsen approach are quite unreliable.

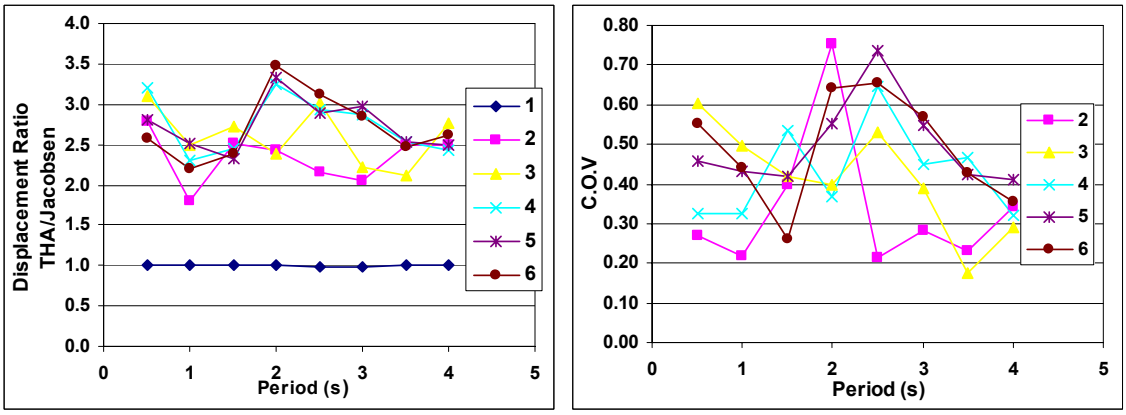

Series represent ductility level from 1 to 6

Figure 7-10 Average Displacement for the elastic perfectly plastic hysteresis model (r=0), Jacobsen Approach

The cause of the large error in the estimation of the displacements is the overestimation of the EVDF by the theoretical equation (6-3). Figure 7-11 clearly shows that the real EVDF is much smaller from the one predicted by the theoretical equation by a factor of 0.3 to 0.5 approximately. The dependency of the

EVDF with period and ductility can still be noticed but the trends are not as clear as in the other models due to the large variation in the results.

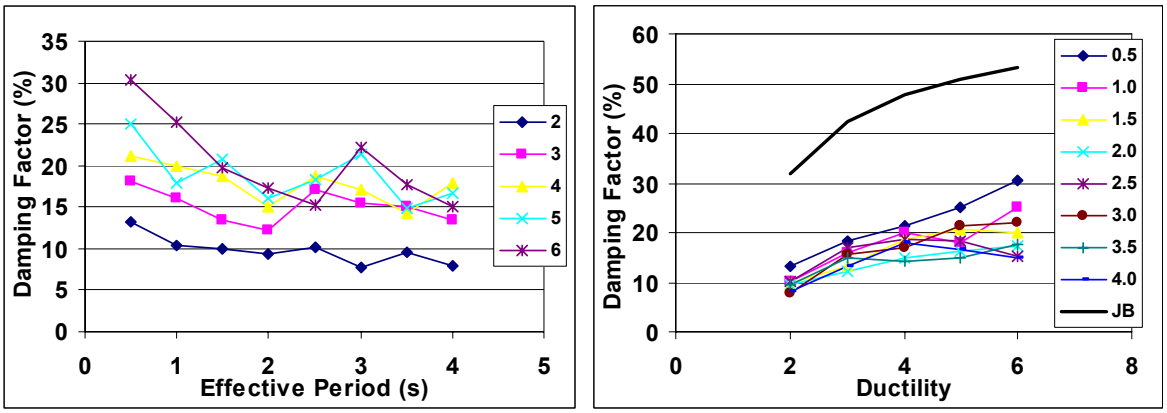

Series represent ductility level from 2 to 6 *Series represent periods from 0.5 to 4.*

Figure 7-11 Equivalent Viscous Damping for the elastic perfectly plastic hysteresis model

The COV of the EVDF is significantly large, which indicates that the estimation of this factor is quite unreliable (Figure 7-12). The large values of the C.O.V and the difficulty to identify clear tendencies of the displacements or the EVDF suggest that the estimation of this factor has to be carried out in a conservative way when this hysteretic model is used.

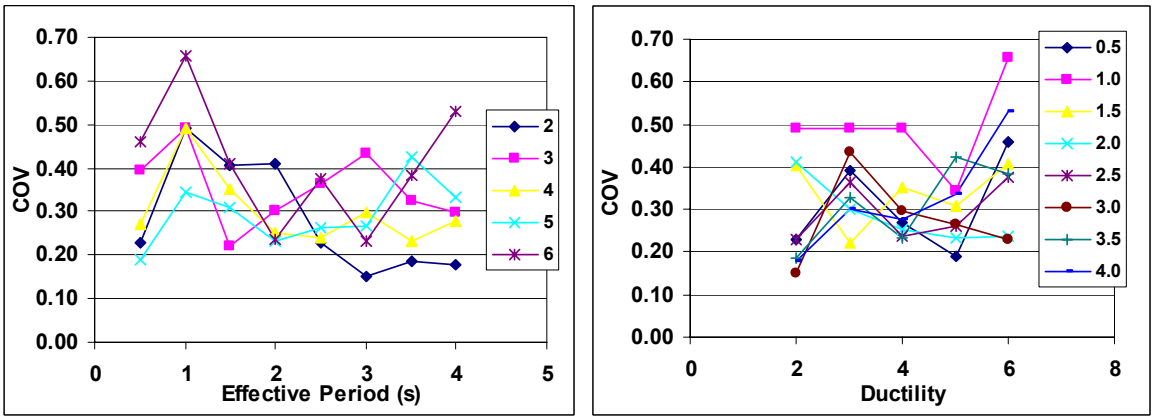

Series represent ductility level from 2 to 6 *Series represent periods from 0.5 to 4.*

Figure 7-12 COV of the Equivalent Viscous Damping Factor for the elastic perfectly plastic hysteretic model.

7.6 RAMBERG OSGOOD HYSTERETIC MODEL

The theoretical damping given by Eq. (6-8) underestimates the effective displacements as shown in Figure 7-13. The time-history displacements are larger for all periods and ductility levels than the initial design displacements. There is also a large C.O.V associated to this ratio which indicates unreliable estimation of the displacements.

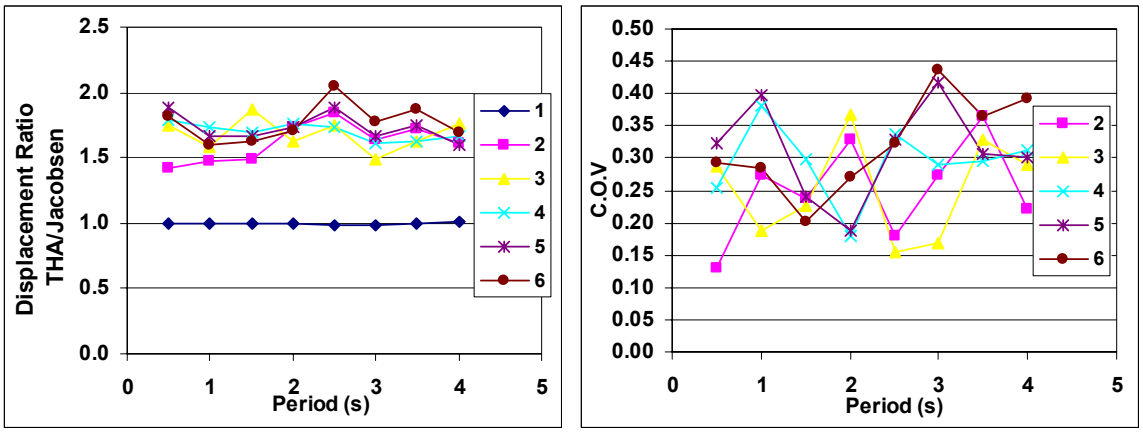

Series represent ductility level from 1 to 6

Figure 7-13 Average Displacement for Ramberg Osgood hysteretic model (γ=7), Jacobsen approach.

The effective EVDF obtained from the iterative procedure tends to show the same behaviour than the rest of the hysteretic models. Even if the average values are slightly disperse, in practical terms it would be possible to have a constant value of damping for all periods for each ductility level. As shown in Figure 7-14, Jacobsen's equation (black line) and (3-16a) proposed by Priestley overestimate the EVDF by a factor of 2 approximately; however, the shape of the variation with ductility is well captured by these equations.

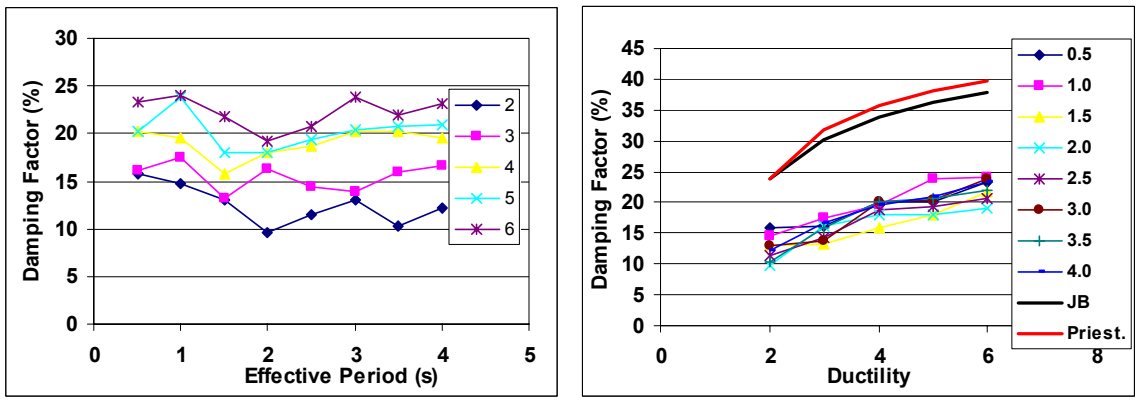

Series represent ductility level from 1 to 6 *Series represent periods from 0.5 to 4.*

Figure 7-14 Equivalent Viscous Damping for the Ramberg - Osgood hysteresis model

The effective damping has a C.O.V that ranges approximately between 0.2 and 0.4, however, for design purposes, it could be taken as 0.3 for all cases given that there is no a particular trend that could allow a differentiated value for each ductility level or effective period.

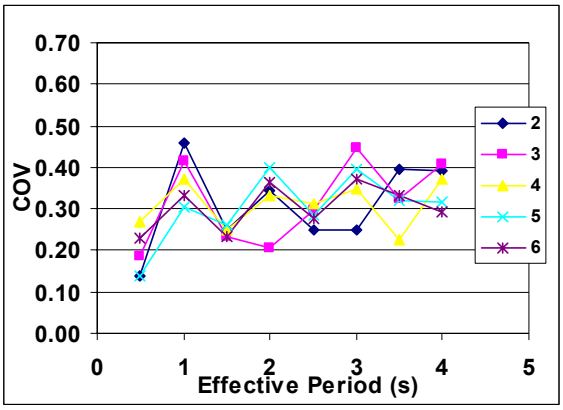

Series represent ductility level from 1 to 6

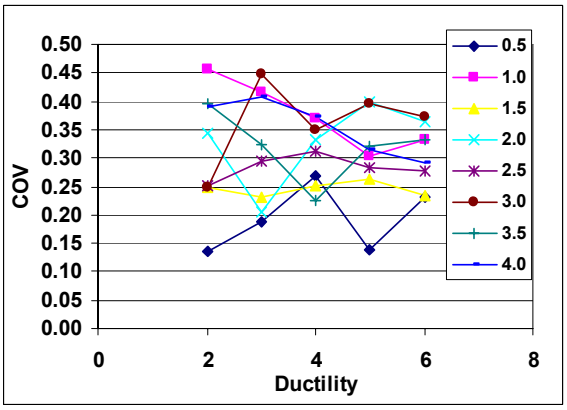

Series represent periods from 0.5 to 4.

Figure 7-15 COV of the Equivalent Viscous Damping Factor for the Ramberg Osgood hysteretic model.

7.7 RING SPRING (FLAG SHAPE) HYSTERETIC MODEL

The THA/ Initial design displacement ratio for this model has some scatter but it indicates that Jacobsens's equation (not presented in the document) tends to give damping factors that produce a overestimation of the displacement for short periods changing to the opposite for large periods (Figure 7-16). The reason for the scatter of the response and the values of the C.O.V is that the effective damping associated to this model is small; hence, a small change of this parameter produces a significant change in terms of displacement.

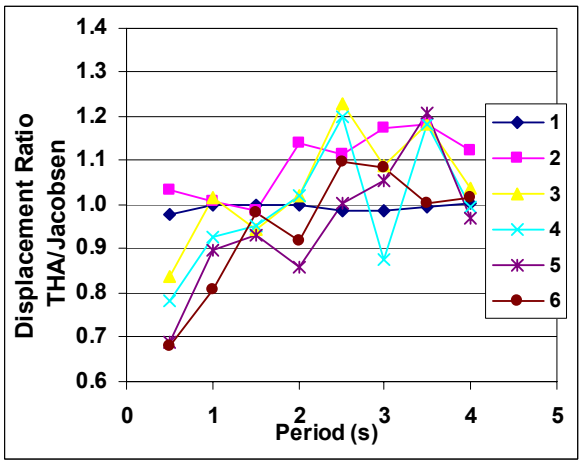

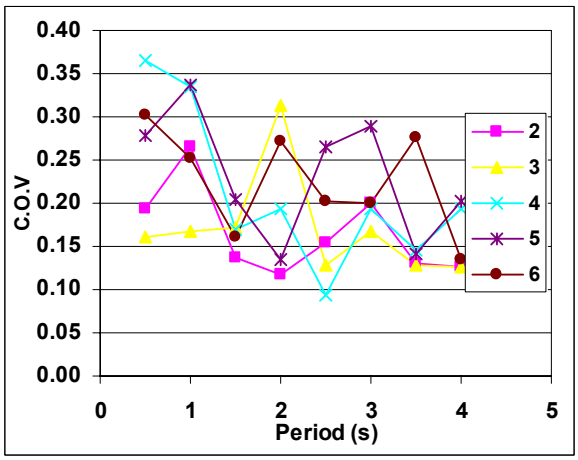

Series represent ductility level from 1 to 6

Figure 7-16 Average Displacement for ring spring model, Jacobsen approach.

Once again, the effective damping obtained presents the same characteristics as the previous models (Figure 7-17). The damping estimated by Jacobsen's approach give an average value of the effective damping. The equation (3-16a) proposed by Priestley underestimates the damping values. However it estimates the shape of the damping in a correct way. For design purposes it would be better to use a modification of this last equation given the complexity of the theoretical equation, for this reason, some corrections will be obtained for it in the next chapter.

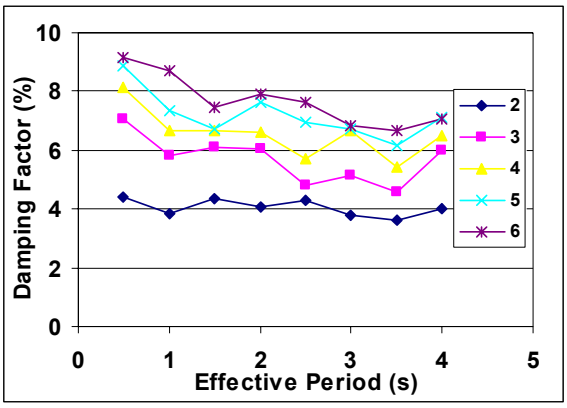

Series represent ductility level from 2 to 6

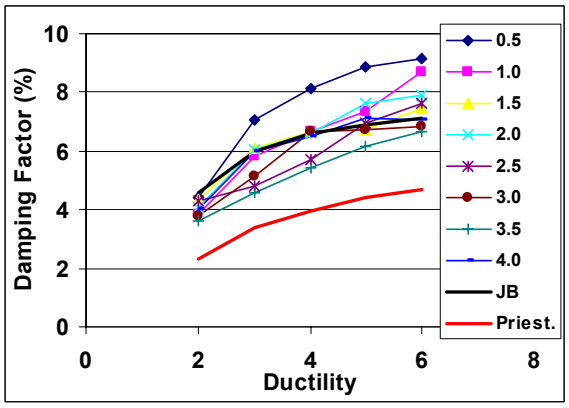

Series represent periods from 0.5 to 4.

Figure 7-17 Equivalent Viscous Damping for the ring spring hysteresis model

The variation of the effective damping is shown in Figure 7-18; where it is possible to observe that there is no evident dependence on ductility or period. A value of 0.20 could be suggested for the C.O.V associated to the mean value.

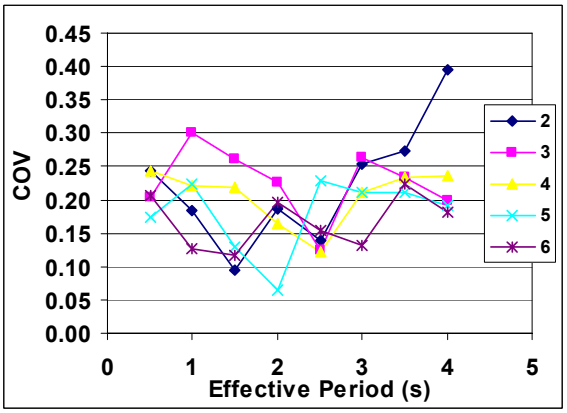

Series represent ductility level from 2 to 6

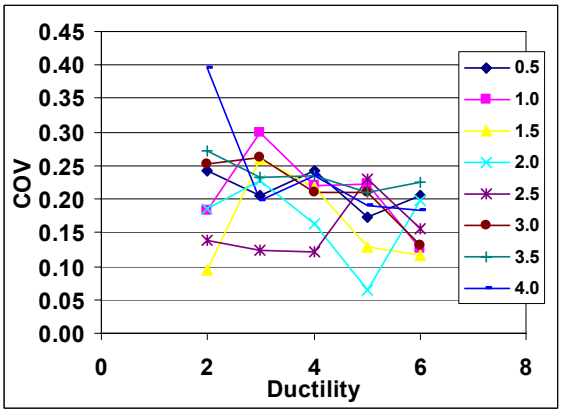

Series represent periods from 0.5 to 4.

Figure 7-18 COV of the Equivalent Viscous Damping Factor for the ring spring hysteretic model.

8 CORRECTED EQUIVALENT VISCOUS DAMPING FACTOR

From the results shown in the previous chapter, it is clear that it is necessary to implement some kind of correction to estimate the EVDF. This correction will depend on the type of hysteretic model, the ductility level and the effective period. Three methods are proposed in this chapter, but only one will be implemented.

8.1 PROPOSED METHODOLOGIES FOR CORRECTION OF THE EQUIVALENT VISCOUS DAMPING FACTOR

8.1.1 Modified equivalent viscous damping equation

This methodology is the one that will be implemented in this study. It consists simply in modifying existing proposed equations to estimate the equivalent viscous damping factor (see section 3.4). Initially, it was proposed to apply a modification factor for the EVDF estimated using Jacobsen's approach; however for most of the hysteretic models, these equations are complicated for practical use in design. Hence, the equations proposed by Priestley were taken as the base for the modified equations proposed here. Finally, the obtained equations have the form:

$$\xi_{effective} = f(\mu)\cdot f(T)\cdot\frac{1}{N} \qquad \textbf{(8-1)}$$

$$\xi_{effective} = \frac{a}{\pi}\cdot\left(1-\frac{1}{\mu^{b}}\right)\cdot\left(1+\frac{1}{(T+c)^{d}}\right)\cdot\frac{1}{N}$$

a,b,c and d are coefficients defined for each hysteretic model μ is the ductility, T is the effective period and N is a normalizing factor; all of which will be explained afterwards.

One important difference of this equation from previous existing proposals is the extra term which is dependant on effective period. This was included given that in the previous chapter it was demonstrated that in general, there is a reduction of the EVDF as period increases.

f(μ) was matched as close as possible to the values of the effective damping for a period 0.5 s. This function is then modified by the *f(T)* in order to match the damping to the other periods.

The normalizing factor (N) is just the result of the expression depending on period (second parenthesis of Eq (8-1)) evaluated for T = 0.5.

$$N = 1 + \frac{1}{(0.5 + c)^d} \tag{8-2}$$

It was found that the parameter c varies between 0.85 and 1, and defines how large is the difference of the EVDF for short effective periods and intermediate periods. The parameter d was found to vary between 2 and 4 and defines how flat the variation of the EVDF at intermediate and large periods is.

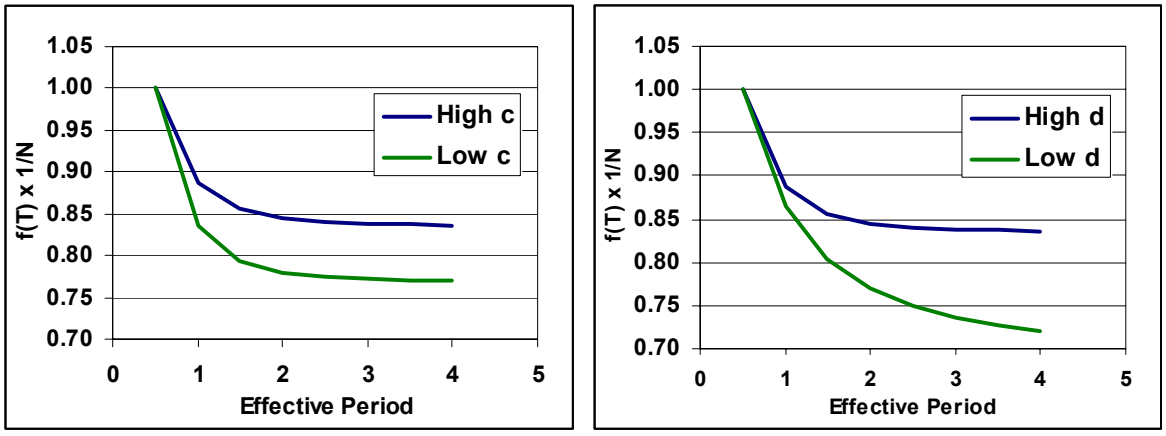

Figure 8-1 Influence of parameters c and d in EVDF.

It is important to mention that the implementation of this approach in DDBD will modify slightly the design process. This is because, in the methodology presented in chapter 2, the damping is obtained directly from the ductility; then, the effective period is obtained for a given target displacement. However, using the modified equation it will be necessary to iterate in order to obtain the period.

The step 4 described in chapter 2 could be as follows:

- Step 4-1 : Select an EVDF randomly or suppose T=0.5s in the modified equation.
- Step 4-2: For the target displacement, obtain the effective period.
- Step 4-3: Compute the EVDF for the period obtained in the previous step and the selected ductility.
- Step 4-4: Repeat the procedure starting at step 4-2 until the effective period converges to the one obtained in the previous loop.

8.1.2 Inelastic Design Response Spectrum

This methodology is based on the displacement response spectrum that is reduced by a factor of ductility, period and hysteretic model (Figure 8-2) [Chopra,1995].

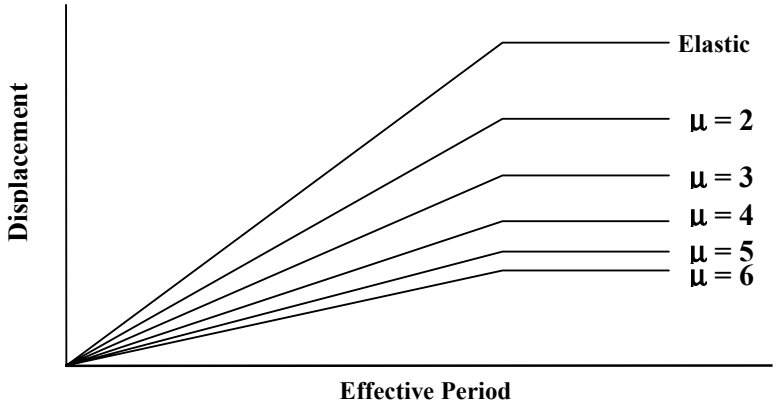

Figure 8-2 Inelastic Design Displacement Response Spectra

8.1.3 Correction Factor For The Elastic Response Spectra

This methodology is based on the reduction of the elastic response spectrum by an empirical factor which depends on damping (Figure 8-3). This technique was used in this study in the iterative process in step 3 using Eq. (5-2) that is repeated here.

$$\Delta_{T,\varepsilon} = \Delta_{T,5} \cdot \sqrt{\frac{7}{2+\varepsilon}}$$

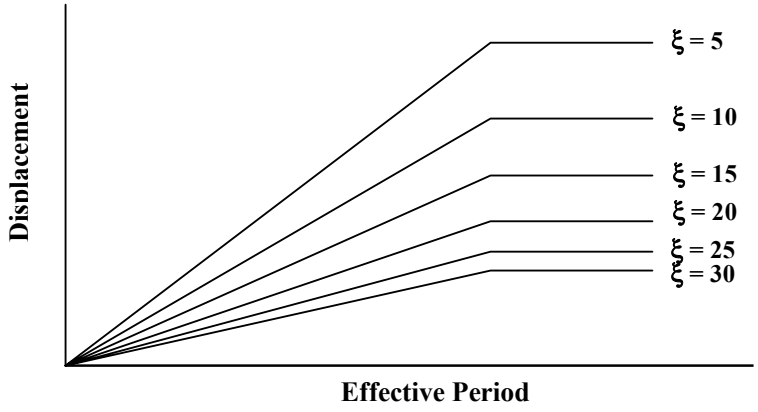

Figure 8-3 Inelastic Design Displacement Response Spectra

Based on the data obtained from the time-history analysis, it would be possible to develop a modified or new expression for the factor η. However; some modifications would be needed in the time-history analysis given that the design elastic response spectrum is based on a 5% initial viscous damping, and for this study this factor was taken as 0.

8.2 MODIFIED EVDF EQUATIONS

The process to obtain the correction factors described in 8.1.1 was carried out for each hysteretic model analyzed. Not all the correction factors depend in the same proportion on the variables (period and ductility) because of different reasons that will be explained for each case.

A perfect match was not possible for all the cases because it was necessary to keep a simple form of the equation. However, in some particular cases, it was necessary to modify the basic form of (8-1) to get a match that could lead to satisfying damping values.

8.2.1 Takeda model (Narrow Type)

As shown previously (Figure 7-2), both Kowalsky's equation based on Jacobsen's approach as given by Eq (6-1) and Priestley's equation ((3-16a) estimate the damping factor with good accuracy by only for a specific effective period. The equation by Priestley was selected given that it estimates with better precision the effective damping obtained by the iterative procedure for a period of 0.5s.

By a trial and error procedure, the constants a and b maintained the same values given by the original Priestley's equation (a = 95 and b = 0.5). Using the same procedure, constants a and b were defined.

Table 8-1 Constant values for the modified Takeda hysteretic model equation (Narrow Type)

Constant	Value
a	95
b	0.5
c	0.85
d	4

Matching to the different ductility levels and effective periods are shown in Figure 8-4. The left plot shows how the EVDF estimated by the modified equation (dashed lines) tends to decrease as the period increase; it also captures the variation with ductility. The right plot shows that the variation between the average value of the EVDF (obtained from the iterative procedure) and the value estimated by the modified equation is for almost all the cases lower than 10% and none of the cases exceeds 22%. It also shows that as the level of ductility increases, the estimation of the EVDF by the modified equation tends to be better.

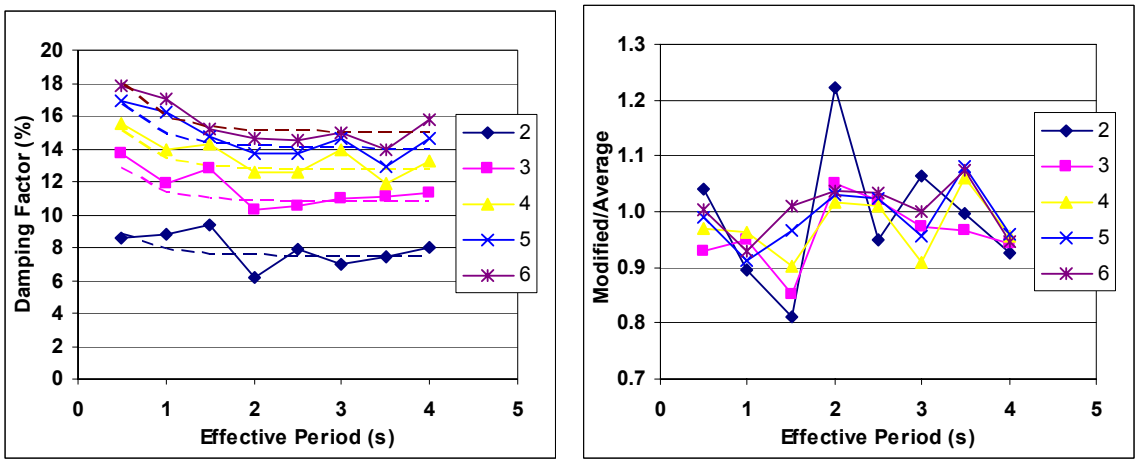

Series represent ductility level from 2 to 6

Figure 8-4 comparison of the EVDF by the modified equation (dashed) and the average effective values (continuous).

It is expected that the displacements obtained using the average value of the correction factor will not have the same coefficient of variation of the EVDF. This is because the variation of this last variable does not occur in the same proportion for displacements. This is true for level of equivalent damping which are not significantly low (see Figure 3-2).

8.2.2 Takeda Model (Fat type)

For this hysteretic model, the equation by Priestley (3-16a) was modified in order to match the effective damping at 0.5 s. The coefficients for the modified equation are shown in table Table 8-2

Table 8-2 Constant values for the modified Takeda hysteretic model equation (Fat Type)

Coefficient	Value
a	130
b	0.5
c	0.85
d	4

The modified equation shows the same behaviour of the "narrow" model (Figure 8-5). However, the EVDF are larger for the fat model and there is also a steeper decrease of the damping as period increases. In this case, the variation of the damping factor obtained with the modified equation and the average of the effective damping is lower than 10% for most of the cases but not larger than 20% in any of them. The variation of the estimated damping factor is still lower than the C.O.V proposed for this model in section 7.3.2.

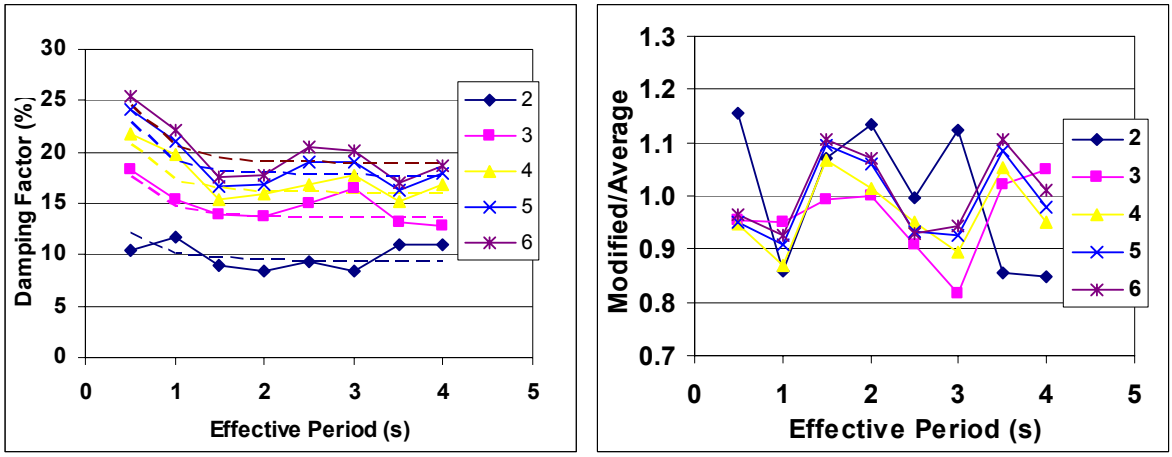

Series represent ductility level from 1 to 6

Figure 8-5 comparison of the EVDF by the modified equation (dashed) and the average effective values (continuous). (fat type)

8.2.3 Bilinear

The effective damping obtained for the bilinear model (section 7.4) show some characteristics which are somehow different from the previous models. The relationship between the EVDF and the ductility tend to have a different shape for ductility levels larger than 4, this is, the EVDF get flatter much quicker than those obtained for the Takeda model. In order to follow this behaviour, it was necessary to adjust the general equation (8-1) as follows:

$$\xi_{effective} = \frac{a}{\pi}\cdot\left(1-\frac{1}{\mu^{b}}-0.1\cdot r\cdot\mu\right)\cdot\left(1+\frac{1}{(T+c)^{d}}\right)\cdot\frac{1}{N} \qquad \textbf{(8-3)}$$

r is the post elastic stiffness coefficient. However, it would be necessary to carry out additional analyses in order to determine for which range of values of *r* this equation is valid. The factors obtained for a,b,c and d are given in Table 8-3.

Table 8-3 Constant values for the bilinear hysteretic model modified equation

Constant	Value
a	160
b	0.5
c	0.85
d	4

The ductility dependent term of the modified equation was adjusted to the effective damping values for a period of 0.5s as shown in Figure 8-6 (red line). The damping is adjusted to the rest of the periods by the normalized factor dependent on period.

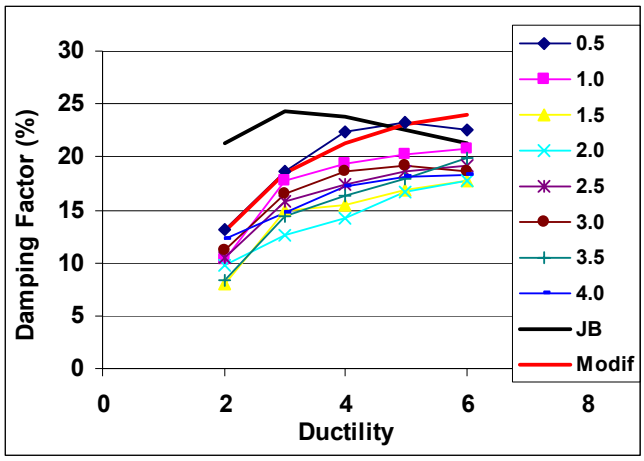

Series represent periods from 0.5 to 4.(Black line Jacobsen's estimation and red line estimation with modified equation)

Figure 8-6 Ductility dependant factor of the modify EVDF equation.

Figure 8-7 shows the comparison between the EVDF from the modified equation and that obtained from the iterative procedure. For this model, the increase of the damping reduces significantly after a ductility level of 4. Right plot shows that the variation between the two approaches is lower than 10% for almost all cases and with only one exception, the variation for all the cases is lower than 20%.

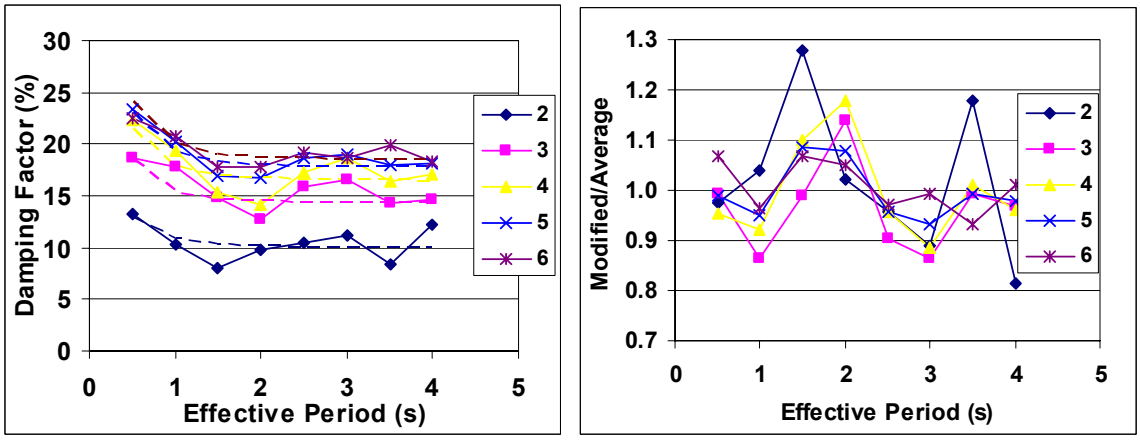

Series represent ductility level from 2 to 6 *Series represent periods from 0.5 to 4.*

Figure 8-7 Comparison of the EVDF by the modified equation (dashed) and the average effective values (continuous).

8.2.4 EPP

The modified equation for the EPP hysteretic model was adjusted to the general form (8-1), reducing significantly the damping obtained by Jacobsen approach Figure 8-2.

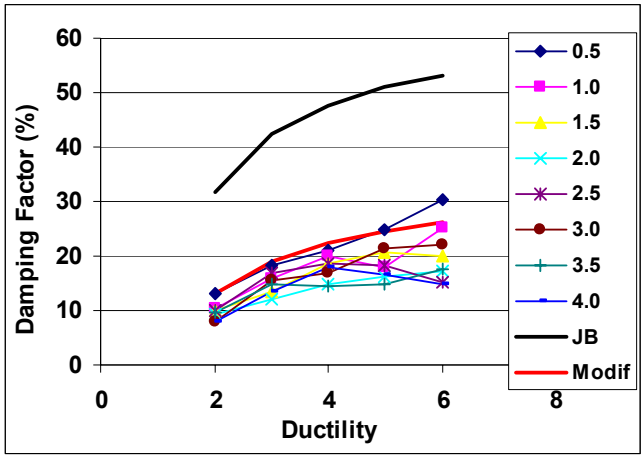

Series represent periods from 0.5 to 4.

Figure 8-8 Comparison of the modified equation (red line) with Jacobsen's approach equation (black line)

The values for the coefficients for Eq. (8-1), are shown in Table 8-4. These coefficients were selected in order to adjust the damping to the effective values for 0.5 s. However, as observed in the figure, the effective damping presents significant scatter.

Table 8-4 Constant values for EPP hysteretic model modified equation.

Constant	Value
a	140
b	0.5
c	0.85
d	2

Comparison between the effective damping and the estimation by the modified equation shows that the variation is larger than in the previous models. However, most of the variation is lower than 15% and for all cases, lower than 22%. This variation is lower than the C.O.V obtained for the effective EVDF as discussed in 7.5.

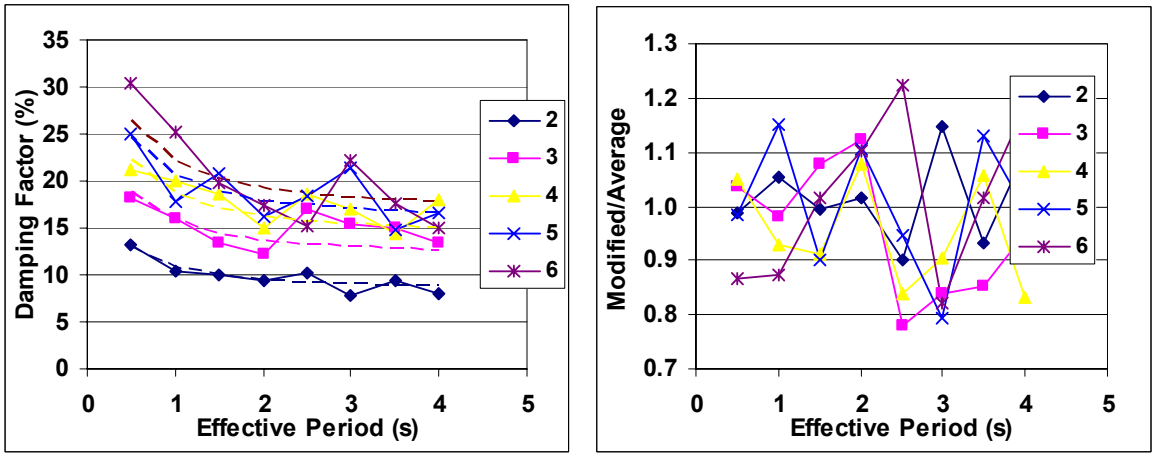

Figure 8-9 Comparison of the EVDF by the modified equation (dashed) and the average effective values (continuous) for EPP model.

8.2.5 Ramberg Osgood

In order to adjust an equation to the Ramber effective damping obtained in 7.6, several coefficients were proved, however, it is difficult to get a simple equation having the from of Eq. (8-1) due to the scatter that the effective damping has. Finally, the coefficients shown in Table 8-5 were selected. The variation shown in Figure 8-10 indicates that almost all the values of damping estimated by the modified equation are lower than ± 20% the effective EVDF. As in the previous models, this variation is lower than the C.O.V obtained in 7.6.

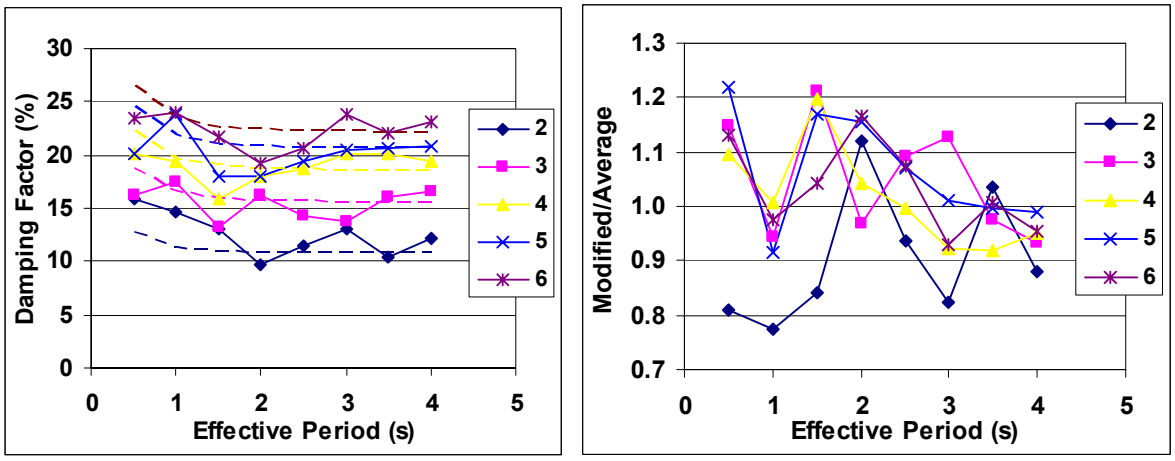

Series represent ductility level from 2 to 6

Figure 8-10 Comparison of the EVDF by the modified equation (dashed) and the average effective values (continuous) for Ramberg model.

Table 8-5 Constant values for Ramberg hysteretic model modified equation.

Constant	Value
a	150
b	0.45
c	1
d	4

8.2.6 Ring Spring

Compared with the equation proposed by Priestley for precast unbonded concrete elements by Eq. (3-16a), the modified equation increase the equivalent damping factor by a factor of 2 for a period of 0.5 sec. The agreement between the effective EVDF and that obtained by the modified equation is better than in the previous models. As shown in Figure 8-11, the variation between the two approaches is lower than 10% for most of the cases but not larger than 15% for any of the cases, which is desirable in particular for this model, given the low effective damping. This is because for this level of effective damping, slight variations of this parameter affect significantly the displacement. Coefficients obtained for Eq. (8-1) are shown in Table 8-6.

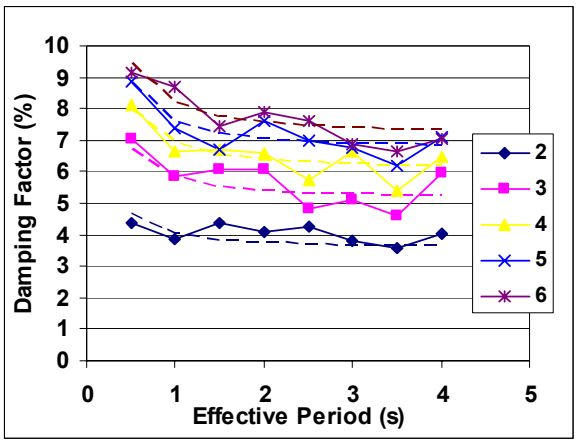

Series represent ductility level from 2 to 6

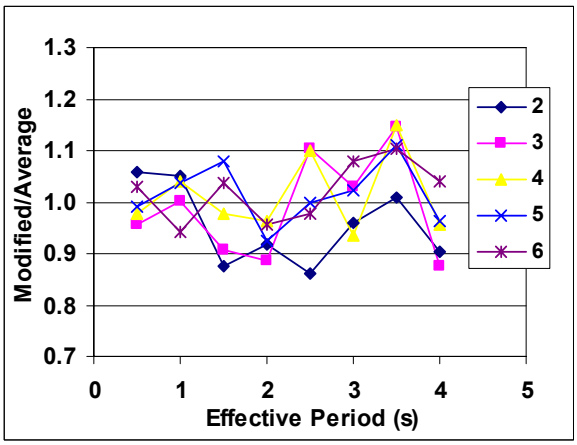

Series represent periods from 0.5 to 4.

Figure 8-11 Comparison of the EVDF by the modified equation (dashed) and the average effective values (continuous) for ring spring model.

Table 8-6 Constant values for ring spring hysteretic model modified equation.

Constant	Value
a	50
b	0.5
c	1
d	3

9 CONCLUSIONS

Design methodologies based on displacements such as the direct displacement based design have demonstrated to be a more rational approach than the methodologies based on forces. However, there are still some improvements that have to be carried out in the design procedure in order to produce more reliable designs.

The traditional method to estimate the equivalent viscous damping for the substitute structure has demonstrated to work adequately for some specific cases of hysteretic models, ductility levels and periods. However, from the results of the analyses carried out in this study, it is possible to conclude that this methodology tends to overestimate the equivalent viscous damping for a large number of cases. This fact cause a significant underestimation of the real displacements making the ductility demands much larger than expected and hence an unconservative design of the members.

The effective equivalent viscous damping factors obtained from the iterative approach have shown to be dependent not only on the ductility but also on period, but not in the same proportion for the different hysteretic models.

These effective factors have a significant variation from the average value; however, the level of variation on displacements is not so significant. This means that it is not necessary to have an exact evaluation of the damping but instead, some coarse evaluation of this factor could lead to accurate levels of displacement.

In order to have a better estimation of the equivalent damping and therefore of the displacements, it is necessary modify the equations obtained using Jacobsen's approach. In order to reduce the complexity for design applications, a general equation was proposed. The coefficients of this equation are modified according to the hysteretic model considered.

The modified equations to estimate the EVDF proposed in this study take into account the effective period. This will require a slight modification of the design procedure of the DDBD. However, the iterative procedure required to apply this equation does not demand complex or time-consuming steps.

Additional analyses have to be carried out in order to evaluate the Jacobsen approach to additional modelling assumptions, such us elastic damping. This means that it will be necessary to repeat the same procedure carried out in this study for a different level of initial viscous damping (probably 5%) whether simple addition of hysteretic and initial elastic damping is appropriate. In carrying out such a study, reference should be made to the relevance of the difference between initial (elastic) period and effective (secant) period at maximum displacement response, as discussed by Priestley and Grant (2004). This difference in period affects the value of elastic damping to be added to the Direct Displacement Based Design Procedure.

REFERENCES

Alvarez J.C "Displacement-based design of continuous concrete bridges under transverse seismic excitation". IUSS Press .Pavia, Italy, in printing. 2004.

Abrahamson, N.A. (1998). "Non-stationary spectral matching program RSPMATCH," PG&E Internal Report, February.

ATC32 [1996] Applied Technology Council "Improved Seismic Design Criteria for California Bridges: Provisional Recommendations" Rept No. ATC-32, Redwood City, California.

Bommer, Julian J and Mendis, Rishmila. "Displacement-Spectra Compatible Acceleration Time-Histories", 11th March 2004.

Borzi B. et al "Inelastic Spectra for Displacement Based Seismoc Design" Soil Dynamics and Earthquake Engineering, 21, 2001, pp 47–61.

Calvi. G.M. "A Displacement-Based Approach for Vulnerability Evaluation of Classes of Buildings" Journal of Earthquake Engineering, Vol. 3, No. 3 (1999) 411-438.

Carr, Athol J. " SIMQKE Generator of Artificial Earthquakes" University of Canterbury, Christchurch, New Zealand. 2002.

Chopra, Anil K. " Dynamics of Structures: Theory and application to earthquake engineering" Prentice Hall, 1995, USA.

EuroCode 8 (1988) 'Structures in seismic regions - Design' Part 1, General and Building. May 1988 Edition, Report EUR 8849 EN, Commission of the European Communities.

Fardis M.N. and Panagiotakos T.B. "Hysteretic Damping of Reinforced Concrete Elements" Elsevier Science Ltd, 1996, Eleventh World Conference on Earthquake Engineering, Paper No 464.

Priestley, M.J.N, and Grant,D.N. "Viscous damping for analysis and design" Journal of Earthquake Engineering. Special Edition, 2005.

Gulkan, P. and Sozen M.A. "Inelastic Responses of Reinforced Concrete Structures to Earthquakes Motions" Procedings of the ACI, Vol 71, No 12, December 1974.

Iwan W.D, Gates N.C. (1979). ' The Effective Period and Damping of a Class of Hysteretic Structures', Earthquake Engineering and Structural Dynamics, V. 7, pp. 199–211.

Judi, H.J., Davidson,B.J. and Fenwick, R.C., "The Direct Displacement Based Design – A Damping Perspective", 12th World Conference on Earthquake Engineering, Auckland, New Zealand, Jan. 2000, Paper No 0330.

Judi, H. Fenwick, R. C., and Davidson, B. J., "Influence of hysteretic form on seismic behaviour of structures", Proceeding on NZSEE Conference, Napier, 2002, paper no.6.5, p10

Kowalsky, Mervyn J.; Ayers, John P. “Investigation of equivalent viscous damping for direct displacement-based design” PEER-2002/02, The Third U.S.-Japan Workshop on Performance-Based Earthquake Engineering Methodology for Reinforced Concrete Building Structures, 16–18 August 2001, Seattle, Washington, Berkeley: Pacific Earthquake Engineering Research Center, University of California, July 2002, pages 173–185.

Miranda, Eduardo and Ruiz-Garcia, Jorge. “ Evaluation of the Approximate Methods to Estimate Maximum Inelastic Displacement Demands” Earthquake Engineering and Structural Dynamics, 2002; 31:539–560.

Pettinga, D, and Priestley, M.J.N. “Dynamic Behaviour of Reinforced Concrete Frames Designed with Direct Displacement-Based Design ”, Journal of Earthquake Engineering, Special Edition, 2005.

Priestley M.J.N. “Myths and Fallacies in Earthquake Engineering, Revisited” The Mallet Milne Lecture, 2003. IUSS Press, Pavia, Italy, May 2003.

Shiabata, A. and M.A. Sozen [1976] “Subtitute-Structure Method for Seismic Design in R/C”. Journal of the Strutural Division, ASCE, New york, USA.

Shunsuke Otani “ Nonlinear analysis of Reinforced Concrete Buildings (Lecture notes)” February 2002, Rose School, Pavia, Italy.

Shunsuke Otani “Hysteresis Models of Reinforced Concrete for earthquake Response Analysis” Journal of Faculty of Engineering, University of Tokyo, Vol XXXVI, No2,1981 pp 407–441.

Structural Engineers Assn. of California (SEAOC), Vision 2000 Committee. April 3, 1995. Performance Based Seismic Engineering of Buildings. J.Soulages, ed. 2 vols. [Sacramento, Calif.]

Sullivan, Tim “The Current Limitations of Displacement Based Design”, MsC Thesis, ROSE School, Pavia, Italy, 2003.